Targeting multiple pro-apoptotic signaling pathways with curcumin in prostate cancer cells

Mariela Rivera[1], Yanilda Ramos[1], Madeline Rodríguez-Valentín[1], Sheila López-Acevedo[1], Luis A. Cubano[1], Jin Zou[2], Qiang Zhang[3], Guangdi Wang[3], Nawal M. Boukli[1] *

1 Department of Microbiology and Immunology, Biomedical Proteomics Facility, Universidad Central del Caribe School of Medicine, Bayamón, Puerto Rico, United States of America, **2** Center for Cancer Research and Therapeutic Development, Clark Atlanta University, Atlanta, Georgia, United States of America, **3** Department of Chemistry, RCMI Cancer Research Center, Xavier University of Louisiana, New Orleans, Louisiana, United States of America

* nawal.boukli@uccaribe.edu

Abstract

Curcumin, an extract from the turmeric rhizome (*Curcuma longa*), is known to exhibit anti-inflammatory, antioxidant, chemopreventive and antitumoral activities against aggressive and recurrent cancers. Accumulative data indicate that curcumin may induce cancer cell death. However, the detailed mechanism underlying its pro-apoptotic and anti-cancer effects remains to be elucidated. In the present study, we examined the signaling pathways triggered by curcumin, specifically, the exact molecular mechanisms of curcumin-induced apoptosis in highly metastatic human prostate cancer cells. The effect of curcumin was evaluated using for the first time in prostate cancer, a gel-free shotgun quantitative proteomic analysis coupled with Tandem Mass Tag isobaric labeling-based-signaling networks. Results were confirmed at the gene expression level by qRT-PCR and at the protein expression level by western blot and flow cytometry. Our findings revealed that curcumin induced an Endoplasmic Reticulum stress-mediated apoptosis in PC3. The mechanisms by which curcumin promoted cell death in these cells were associated with cell cycle arrest, increased reactive oxygen species, autophagy and the Unfolded Protein Response. Furthermore, the upregulation of ER stress was measured using key indicators of ER stress: Glucose-Regulated Protein 78, Inositol-Requiring Enzyme 1 alpha, Protein Disulfide isomerase and Calreticulin. Chronic ER stress induction was concomitant with the upregulation of pro-apoptotic markers (caspases 3,9,12) and Poly (ADP-ribose) polymerase. The downregulated proteins include anti-apoptotic and anti-tumor markers, supporting their curcumin-induced pro-apoptotic role in prostate cancer cells. Taken together, these data suggest that curcumin may serve as a promising anticancer agent by inducing a chronic ER stress mediated cell death and activation of cell cycle arrest, UPR, autophagy and oxidative stress responses.

Introduction

Prostate cancer (Pca) is one of the most common malignancies and the second leading cause of tumor-related mortality in American males [1]. Conventional therapies produce a high rate of cure for patients with localized prostate cancer by surgical therapy, but there is no cure once the disease has spread beyond the prostate. In spite of advances in chemotherapy, Pca therapies have not been completely successful in eradicating the disease and have been found to be toxic to normal patient cells [2], thus, new agents are needed to selectively kill cancer cells. For the past several centuries, natural products/dietary phytochemical compounds have been used in the treatment of cancer and are still the major source of new drug development. Among nontoxic natural compounds, curcumin, the active ingredient in *Curcuma longa*, is known for its ability to target cancer cells and for its therapeutic and anti-invasive properties [3–5]. Curcumin is a natural phenolic compound that has been studied for its anti-proliferative, anti-inflammatory, and anti-oxidative properties [6, 7]. The purpose of the present study was to investigate the effects of curcumin on highly metastatic human prostate cancer cells (PC3) and the mechanisms underlying its anticancer and anti-apoptotic properties. We speculate that curcumin alters the expression of proteins associated with pro-apoptotic mechanisms, one of them being chronic ER stress mediated cell death. When the cell undergoes cytotoxic conditions, protein misfolding occurs, leading to unfolded proteins aggregating in the ER. To correct misfolding, the cell triggers the unfolded protein response (UPR). Chaperones and folding enzymes, such as the 78-kD Glucose-Regulated Protein (GRP78), protein disulfide isomerase (PDI), eukaryotic translation initiation factor 2 alpha (eIF2α), and calreticulin (CALR) have been shown to play a key role in this process. Under acute ER stress conditions, the cell resorts to survival, while chronic ER stress triggers cell death. The microenvironments of cancerous cells have been shown to exert ER stress resistance, which is required for the survival and growth of tumors. However, prolonged or severe ER stress may ultimately overwhelm the cellular protective mechanisms, triggering cell death through specific programmed cell death pathways [8]. Apoptosis prompted by chronic ER stress can occur through the intrinsic pathway, which is activated by the transcription factor CCAAT-enhancer-binding protein homologous protein (CHOP) and subsequent caspase activation [3].

UPR and ER stress may induce the activation of alternative stress pathways such as autophagy, reactive oxygen species (ROS) responses, cell cycle arrest, among others [9]. Autophagy is initiated by encapsulation of cytoplasmic components (proteins and organelles) within isolation membranes to form autophagosomes. These structures eventually fuse with lysosomes and the cargo is degraded. Accumulative data indicated that the UPR may induce autophagy and that it can alleviate the UPR or promote cell death [10, 11]. However, the detailed mechanism of interplay between autophagy and UPR remains to be fully understood. Activation of the double-stranded RNA-activated protein kinase (PKR)-like endoplasmic reticulum (ER) kinase (PERK)–eukaryotic translation initiation factor 2 alpha (eIF2α)–activating transcription factor 4 (ATF4) pathway upregulates the expression of a large set of autophagy genes. Functionally, autophagy promotes cell survival, increases energy supply, and mediates innate immune responses. Nevertheless, autophagy can also be associated with cell death and apoptosis, depending on the cell stress level.

Reactive Oxygen Species (ROS) is referred to oxygen containing reactive molecules and free radicals derived from metabolism of oxygen and is responsible for causing significant damages in the cell, increasing the intracellular amount of mitochondrial biogenesis or responses. These elevated ROS mediate adverse consequences in cells and have been linked to ER stress and the UPR [12]. In a stressed ER, dysregulated disulfide bond formation and breakage may result in reactive oxygen species (ROS) accumulation and cause oxidative stress

[13]. This is followed by Ca^{2+} release from the ER and mitochondrial ROS production creating a vicious cycle that impairs cellular homeostasis and induces apoptosis. Given the deleterious impact of oxidative stress induced during protein misfolding in the ER, eukaryotic cells have evolved antioxidative stress responses to restore cellular redox homeostasis. The PERK branch of the UPR induces antioxidative stress response genes, and is responsible for uncoupling mitochondrial protein 2 [14]. In settings of chronic and prolonged ER stress conditions, these mechanisms may lead to apoptosis induction [15]. The results obtained in the present study indicate that curcumin induced a chronic ER stress mediated cell death, and activated an orchestrated mechanism associated with cell cycle arrest, UPR, autophagy and oxidative stress response.

The identification of key differentially expressed proteins has been successfully applied to understand curcumin's effect on PCa by means of a gel-free shotgun quantitative proteomic analysis coupled with Tandem Mass Tag Isobaric Labeling. The results were validated using qRT-PCR, flow cytometry and western blotting. Results from these analyses provide insights into curcumin mechanisms and suggest that curcumin induced specifically a chronic ER stress mediated cell death in PC3. We speculate that curcumin induces apoptosis in PC3 by activating cell cycle arrest, oxidative stress and UPR.

Materials and methods

Cell culture

The PC3 cell line (ATCC) was derived from a bone metastasis from a grade IV prostatic adenocarcinoma patient. PC3 cells were cultured in complete F-12K medium supplemented with 10% fetal bovine serum (FBS, Invitrogen, Grand Island, NY) and 1% penicillin/streptomycin (Invitrogen) at a density of 5 x 10^4 cells/cm^2 in 75cm^2 culture flasks (BD Biosciences). Cells were maintained in a cell culture incubator at 37°C in a humidified atmosphere with 5% CO_2.

Prostate cancer cell (PC3) treatment with curcumin

Approximately 2 x 10^6 PC3 cells were seeded in 75-cm^2 culture flasks in supplemented F-12K medium, allowed to adhere for 24 hours, and maintained in a humidified atmosphere with 5% CO_2 and 37°C. Curcumin was added at a concentration of 5 µg/ml, as previously published in collaboration with Kurapati et al. [16]. This concentration was chosen since it showed significant inhibition of colony formation in clonogenic assays at 5 µg/mL in PC3 cells. PC3 cells were incubated for 72 hours while control cells were treated with 0.4% (by volume) dimethyl sulfoxide (DMSO, Sigma-Aldrich, St. Louis, MO) for 72 hours as previously described [17]. Curcumin was obtained from Sigma Aldrich and dissolved in DMSO at a concentration of 1mg/ml.

Acridine orange analysis

Acridine orange (Sigma Aldrich) was used to assess autophagy. Cells were seeded in 25cm^2 flasks and treated with curcumin or DMSO for three days, cells were washed with PBS and stained with 5µg/ml of acridine orange. Images were acquired on an Olympus IX70 inverted fluorescent microscope (Olympus America Inc., Center Valley, NJ), using the Q Capture Pro software (QImaging, Surrey, Canada).

Cell viability by ReadiDrop 7-AAD

7-aminoactinomycin D (BioRad, Hercules CA), was used to determine cell viability after treatment with either curcumin or DMSO. The manufacturer's protocol was followed. Stained cells

were measured by flow cytometry with a FACSCanto II (Becton Dickinson, San Jose, CA, USA). Data analysis was performed using FlowJo data analysis software v. 10 (Ashland, OR).

Gel-free isobaric labeling tandem mass tag quantitative proteomic profiling of PC3 cells treated with curcumin

Cell lysis and protein extraction.   Cells were plated on 150 cm^2 culture plates at a cell density of 5×10^6 and treated the following day with 5 µg/ml curcumin for 72 h. Cells treated with DMSO were used as controls. Proteins were extracted with RIPA (1.5 M Tris pH 8.8, 1.75 g NaCl, 2 mL sodium dodecyl sulfate 10%, 2 mL Triton X-100; all reagents from Thermo Fisher Scientific, (Waltham, MA). The cells were incubated on ice for 30 min, followed by 5 min sonication and centrifugation at 20,000 rpm for 5 min in preparation for protein extraction. Protein concentration was calculated on microtiter plates by measuring the absorbance at 595 nm of samples containing Bradford reagent (Bio-Rad Laboratories, Hercules, CA) supplemented with phosphatase and protease inhibitor cocktail (Roche Molecular Biochemicals, Indianapolis, IN).

Reduction, alkylation, and trypsin digestion.   Aliquots with 100 mg of proteins from each sample were added to 100 ml of 200 mM triethyl ammonium bicarbonate TEAB (Sigma-Aldrich, St. Louis, MO). Reduction was performed by adding 5 ml of 200 mM tris (2-carboxyethyl) phosphine TCEP (Sigma-Aldrich, St. Louis, MO) to each replicate and incubating for 1 h at 55˚C. Alkylation was carried out by adding 5 ml of 375 mM iodoacetamide (Bio-Rad Laboratories, Hercules, CA) to each sample and incubating for 30 min at room temperature. After alkylation, 1 ml of pre-chilled acetone was added and precipitation was allowed to proceed for 3 h at 20˚C. Acetone-precipitated protein pellets were suspended in 100 ml of 200 mM TEAB and digested overnight at 37˚C with 2.5 µg of sequencing grade modified trypsin (Promega Corp., Madison, WI) as previously described [18].

Isobaric labeling with tandem mass tag.   The non-gel isobaric labeling Tandem Mass Tag (TMT) quantitative proteomic approach was performed as previously described in Burton et al, 2016 [18]. TMTs with varying molecular weights (126–131 Da) (Thermo Fisher Scientific, Waltham, MA) were used as isobaric labels to determine differential protein expression between PC3 control cells treated with DMSO (0.4%) and PC3 cells treated with 5µg/ml curcumin. According to the manufacturer's protocols, the six digested samples were individually labeled with TMT reagents as follows. Three control (DMSO-treated) samples, TMT-126 (batch 1), TMT-127 (batch 2), and TMT-128 (batch 3); and three curcumin-treated samples, TMT-129 (batch 1), TMT-130 (batch 2), and TMT-131 (batch 3). The labeled peptide mixtures were combined in equal ratios. The TMT-labeled peptide mixture was fractionated with a strong cation exchange SCX column (Thermo Fisher Scientific, Waltham, MA) on a Shimadzu 2010 high performance liquid chromatography (HPLC) equipped with an ultraviolet detector (Shimadzu, Columbia, MD) and a mobile phase consisting of buffer A (5 mM KH$_2$PO$_4$, 25% acetonitrile, pH 2.8) and buffer B (buffer A plus 350 mM KCl). The column was equilibrated with buffer A for 30 min before sample injection. A mobile phase gradient at a flow rate of 1.0 ml/min was set as follows: 1) 0 ~ 10 min: 0% buffer B; 2) 10 ~ 40 min: 0 ~ 25% buffer B; 3) 40 ~ 45 min: 25 ~ 100% buffer B; 4) 45 ~ 50 min: 100% buffer B; 5) 50 ~ 60 min: 100 ~ 0% buffer B; and 6) 60 ~ 90 min: 0% buffer B. Sixty fractions were initially collected, lyophilized, and combined into 10 final fractions based on SCX chromatogram peaks.

Desalination of fractionated samples.   A C$_{18}$ solid phase extraction SPE column (Thermo Fisher Scientific, Waltham, MA) was used to desalt all collected fractions as previously described. Briefly, the 10 combined fractions were each adjusted to a final volume of 1 ml in a 0.25% trifluoroacetic acid (TFA) aqueous solution. The C$_{18}$ SPE column was preconditioned

with 1 ml acetonitrile and eluted in approximately 3 min before it was rinsed with 3×1 ml 0.25% TFA. The fractions were loaded on to the top of the SPE cartridge column slowly, and were reloaded once again to decrease lost peptide during column binding. Columns were washed with 4×1 ml 0.25% TFA aliquots before the peptides were eluted with 3×400 µl 80% acetonitrile/0.1% formic acid (aqueous). The eluted samples were lyophilized prior to the liquid chromatography mass spectrometry LC-MS/MS analysis.

LC-MS/MS analysis.   Peptides were analyzed on an LTQ-Orbitrap XL (Thermo Fisher Scientific, Waltham, MA) instrument interfaced with an Ultimate 3000 Dionex LC system (Dionex, Sunnyvale, CA). High mass resolution was utilized for peptide identification and high-energy collision dissociation (HCD) was used for reporter ion quantification as previously described [18]. Briefly, the reverse phase LC system contained a peptide Cap-Trap cartridge (0.5×2 mm) (Michrom BioResources, Auburn, CA) and a pre-packed BioBasic C_{18} PicoFrit analytical column (75 µm i.d. $\times$ 15 cm length, New Objective, Woburn, MA) fitted with a FortisTip emitter tip. Samples were loaded onto the trap cartridge and washed with mobile phase A (98% H_2O, 2% acetonitrile, and 0.1% formic acid) for concentration and desalting. Peptides were eluted over 180 min from the analytical column via the trap cartridge by using a linear gradient of 6 to 100% mobile phase B (20% H_2O, 80% acetonitrile, and 0.1% formic acid) at a flow rate of 0.3 µl/min. The Orbitrap mass spectrometer was operated in a data-dependent mode in which each full MS scan (60,000 resolving power) was followed by six MS/MS scans where the three most abundant molecular ions were dynamically selected and fragmented by collision-induced dissociation with a normalized collision energy of 35% and subsequently scanned by HCD-MS^2 with a collision energy of 45% as previously described [18]. Only the 2+, 3+, and 4+ ions were selected for fragmentation by collision-induced dissociation and HCD.

Database search and TMT quantification.   The protein search algorithm SEQUEST was used to identify unique protein peptides using the Proteome Discoverer data processing software (version 1.2, Thermo Fisher Scientific, Waltham, MA). The ratios of TMT reporter ion abundances in MS/MS spectra generated by HCD from raw data sets were used For TMT quantification. Fold changes in proteins between control and treatment were calculated as previously described [18].

Intracellular staining by flow cytometry

Cells were blocked for 10 minutes with 1% of BSA/PBS and incubated for 30 minutes in ice with the use of the rabbit polyclonal antibody against human cleaved caspase 3 (1:800) for experiments assessing cell death and p-eIF2α (1:100) for experiments assessing translational attenuation (Cell Signaling Technology, Danvers, MA). Cells were acquired and analyzed on a FACSCanto II and FlowJo software (TreeStar, Ashland, OR).

Cleaved caspase-3 sandwich ELISA

Quantification of cleaved caspase-3 was performed using the PathScan Cleaved Caspase-3 (Asp175) sandwich ELISA kit (Cell Signaling) according to manufacturer's recommendations.

Intracellular oxidative species

Intracellular oxidation levels were determined by 2',7'-dichlorodihydrofluorescein diacetate staining (H2DCFDA; Molecular Probes, Eugene, OR) which in the presence of intracellular ROS is oxidized to highly fluorescent 2′,7′-dichlorofluorescein (DCF). After treatment with curcumin or DMSO, cells were incubated at 37˚C for 30 minutes with 1µM of HD2CFDA.

The dye was removed and cells were washed once with PBS and analyzed on a FACSCanto II and FlowJo software (TreeStar, Ashland, OR).

Cell cycle analysis

For cell cycle assays, 1×10^6 curcumin treated PC3 and control cells were fixed with 70% ethanol solution at 4°C for 1 hour, then washed with 1X PBS, and incubated with a 0.2 mg/mL RNase A (Sigma Aldrich, St. Lois, MO) for 1 h at 37°C. The cell suspension was supplemented with 10 µg/mL of propidium iodide (Sigma Aldrich, St. Lois, MO) and incubated at 4°C for 1 hour protected from light. Samples were analyzed on a FACSCanto II and FlowJo software (TreeStar, Ashland, OR).

Western blot

Proteins were extracted with RIPA buffer (1.5 M Tris pH 8.8, 1.75 g NaCl, 2 mL of 10% sodium dodecyl sulfate, 2 mL Triton X-100; all reagents from Fisher Scientific) plus a protease inhibitor cocktail. Protein quantification was performed with the Pierce™ BCA Protein Assay Kit (Thermo Fisher Scientific, Waltham, MA). The samples absorbance was read and analyzed using the SoftMax Pro software (Molecular Devices, Sunnyvale, CA) coupled to a VersaMax Tunable microplate reader (Molecular Devices, Sunnyvale, CA) detecting at 562 nm excitation. Proteins were then analyzed by SDS-PAGE and transferred to a PVDF membrane. Membranes were blocked with 5% non-fat dry milk in Tris-buffered saline and Tween 20 (TBST) and incubated with primary antibodies overnight at 4°C. The primary antibodies used in this experiment were: anti-casp 12 (1:1000 dilution; Abcam, Cambridge, MA), anti-Ire1α (1:1000, Cell Signaling Technology), anti-GRP78 (1:1000, Cell Signaling Technology), anti-calreticulin (1:1000, Abcam), anti-PARP (1:1000, Cell Signaling Technology) and anti-LC3B (1:1000, Cell Signaling Technology). To confirm equal loading, blots were stained with 0.1% India ink. Horseradish peroxidase-conjugated secondary antibodies were used, and protein bands were visualized by a chemiluminescent method using the SuperSignal West Femto Maximum Sensitivity Substrate kit (Thermo Fisher Scientific, Waltham, MA). Images were analyzed with the ImageJ software (Bethesda, MD, USA) by comparing band densities (peak percent).

Quantitative real-time PCR

SYBR green qRT-PCR gene expression assays was performed for Caspase-3 (*CASP3*) and Caspase-9 (*CASP9*) genes. Amplification was carried out in a Bio-Rad CFX96 Touch real-time PCR detection system (Bio-Rad, Hercules, CA) using the following program: 10 minutes at 95°C, 50 cycles of 15 seconds at 95°C, and 1 minute at the gene-specific annealing temperature. The gene-specific primers were: *CASP-3* forward 5′-AAATGAATGGGCTGAGCTGC-3′; *CASP-3* reverse 5′-GCGTATGGAGAAATGGGCTG-3′; CASP-9 forward 5′-AAGTGACCCT CCCAAGTAGC-3′; CASP-9 reverse 5′-GAGACCTAACCTCCCTGAGC-3′. The gene expression level was defined as the threshold cycle number (CT). Mean fold changes in expression of the target genes were calculated using the comparative CT method (RU, 2–ΔΔCt). All data were controlled for the quantity of RNA input by *18S* forward 5′-GGCCCTGTAATTGGAAT GAGTC-3′; *18S* reverse 5′-CCAAGATCCAACTACGAGCTT-3′ serving as the endogenous control and for normalization.

Statistical analysis

Cytoxicity assays, quantitative PCR and proteomics experiments were performed in biological and technical triplicates, using separate trials with similar results. Statistical analysis was

performed using two-way ANOVA and unpaired t-tests, as appropriate, by means of Graph-Pad PRISM v6.03 statistical software (GraphPad Software, La Jolla, CA). p<0.05 was considered statistically significant.

Results

Proteomic profiling of PC3 cells treated with curcumin: A TMT isobaric-labeling quantitative gel free proteomic approach

The differential expression of proteins between untreated (0.4% DMSO) and treated (5 μg/ml curcumin) PC3 cells was determined based upon an isobaric labeling, TMT, quantitative proteomic approach for further validation and identification of novel proteins. Comparative quantitative proteomics identified over 926 proteins (S1 Table) in control and treated PC3 cell lysates, out of which 330 proteins were differentially expressed. Proteins with a statistically significant fold change ≥ 1.2 or ≤ -1.2-fold were considered differentially expressed. The detailed information including gene symbol, gene name, fold change, p value, molecular weight and calculated pI are shown in Table 1. Because it was not feasible to discuss all identified proteins (926), the selection criteria were based on significance in terms of fold change.

Curcumin-treated PC3 cells expressed 146 upregulated and 184 downregulated proteins when compared with control PC3 cells (treated with DMSO). Of the identified proteins upregulated by curcumin figure ER stress markers such as GRP78 (Glucose Regulated Protein 78kDa or HSPA5) and PDI. These two proteins need special mention since they are involved in sensing and respond to the accumulation of unfolded or misfolded proteins in the ER. GRP78 and the PDI family were upregulated by 1.69 and ≥1.25-fold respectively as determined by the TMT 6-plex quantitation method. Curcumin treatment led to the upregulation of several ER stress markers and chaperones such as HSPA9 and ERP29 with significant fold change levels of 1.19 and 1.27, respectively in PC3 cells. Among other upregulated proteins related to ER stress figure eukaryotic translation initiation factor 2A (EIF2A), with a significant fold change of 1.25, and the ER stress pro-apoptotic protein calnexin (CANX) [19], which was significantly increased to 1.19-fold relative expression in the curcumin-treatment group as compared to control ($^*p ≤ 0.05$; $n = 3$) (Table 1). The differentially expressed proteins included downregulated anti-oxidant markers such as peroxiredoxin 6 (PRDX6) and protein DJ-1 (PARK7) with significant fold changes of –1.39 and –1.51, respectively, correlating with the upregulation of reactive oxygen species markers such as annexin A1 (ANXA1) [20] and sulfiredoxin-1 (SRXN1), with fold changes of 1.45 and 1.38, respectively, in curcumin-treated PC3 cells. Furthermore, curcumin altered the expression of pro-apoptotic markers (annexin A5, PGRMC1 and vimentin), anti-apoptotic protein signatures (Inorganic pyrophosphatase and VAMP-associated protein A); cell cycle, migration and proliferation proteins (cyclin-dependent kinase 1, heat shock protein HSP 90-alpha and beta, endoplasmic reticulum protein 29, Ras-related protein Rap-2b, PPP1CA); endoplasmic-reticulum-associated degradation (ERAD) activation (PMPCA, PSMB2, PSMC1, PSMD2); oxidative stress regulators (PARK7, PDZ and LIM domain protein 1, sulfiredoxin); cytoskeleton and transport proteins (vimentin, profilin, myosin, dynamin, destrin, filamin B, tubulin and transmembrane emp24) and autophagy related proteins (Rab GDP dissociation inhibitor beta, protein DJ-1 and ubiquitin-like modifier-activating enzyme 1) in PC3 cells.

Curcumin extract reduces cell viability and induces a cell cycle arrest in PC3 cells

As previously reported by Kurapati et al. [16], *C. longa* showed significant inhibition of colony formation in clonogenic assays at 5 μg/mL in PC3 cells, a dose we chose in our assays. The

Table 1. Overexpressed proteins identified in PC3 cells treated with curcumin and arranged in decreasing fold change order.

Upregulated Proteins

Gene Symbol	Protein Name	Fold Change	P value	MW (kDa)	pI
SLC1A5	solute carrier family 1 (neutral amino acid transporter), member 5	2.03	5.69E-05	56.56	5.48
TBC1D10B	TBC1 domain family, member 10B	1.93	1.41E-06	87.14	9.19
MRPS17	mitochondrial ribosomal protein S17	1.91	1.94E-04	14.49	9.85
YBX1	Y box binding protein 1	1.75	2.27E-05	34.65	7.53
HSPA5	heat shock 70kDa protein 5 (GRP78)	1.69	4.98E-07	72.29	5.16
DAK	dihydroxyacetone kinase 2 homolog (S. cerevisiae)	1.61	1.12E-01	58.91	7.49
PRPF40A	PRP40 pre-mRNA processing factor 40 homolog A (S. cerevisiae)	1.61	1.53E-04	95.04	7.36
EEF1G	eukaryotic translation elongation factor 1 gamma	1.59	8.06E-05	24.09	7.05
SRSF1	serine/arginine-rich splicing factor 1	1.59	2.45E-03	22.45	7.94
YARS	tyrosyl-tRNA synthetase	1.59	1.29E-05	59.11	7.05
SLC3A2	solute carrier family 3 (amino acid transporter heavy chain), member 2	1.57	1.93E-04	55.9	5.17
SNRPF	small nuclear ribonucleoprotein polypeptide F	1.56	6.28E-03	9.72	4.67
HIST1H4A	Histone H4	1.53	6.66E-05	11.36	11.4
HSPE1	heat shock 10kDa protein 1 (chaperonin 10)	1.51	3.48E-06	10.92	8.92
EFTUD2	elongation factor Tu GTP binding domain containing 2	1.5	3.80E-03	105.32	5.22
SF3B1	splicing factor 3b, subunit 1, 155kDa	1.5	9.97E-04	145.74	7.09
APOL1	apolipoprotein L, 1	1.49	2.20E-08	18.1	5.43
HSP90B1	heat shock protein 90kDa beta (Grp94), member 1	1.48	2.54E-05	92.41	4.84
PLCH1	phospholipase C, eta 1	1.48	2.44E-07	114.43	7.64
ABHD10	abhydrolase domain containing 10	1.47	1.31E-05	16.9	6.73
ANXA1	annexin A1	1.45	2.12E-05	38.69	7.02
LAMP2	lysosomal-associated membrane protein 2	1.45	7.05E-04	39.79	5.67
STC2	stanniocalcin 2	1.45	2.22E-03	33.23	7.3
GRPEL1	GrpE-like 1, mitochondrial (E. coli)	1.44	2.61E-05	21.89	8.62
HNRNPAB	heterogeneous nuclear ribonucleoprotein A/B	1.44	1.69E-05	30.28	7.91
TPD52L2	tumor protein D52-like 2	1.44	1.73E-05	19.89	5.48
CYB5B	cytochrome b5 type B (outer mitochondrial membrane)	1.42	1.28E-02	14.84	6.19
DDX17	DEAD (Asp-Glu-Ala-Asp) box helicase 17	1.42	4.12E-02	47.53	7.66
KPNA3	karyopherin alpha 3 (importin alpha 4)	1.42	8.36E-02	10	3.95
AGR2	anterior gradient 2	1.4	1.77E-04	19.97	9
ANXA7	annexin A7	1.4	8.45E-05	37.78	7.18
EEF1E1	eukaryotic translation elongation factor 1 epsilon 1	1.4	3.45E-03	5.88	8.62
FUS	fused in sarcoma	1.4	2.26E-05	15.23	9.41
FLNB	filamin B, beta	1.39	1.44E-04	275.5	5.78
KHSRP	KH-type splicing regulatory protein	1.39	1.06E-04	72.85	7.9
ALYREF	Aly/REF export factor	1.38	1.12E-04	26.87	11.2
CLTA	clathrin, light chain A	1.38	3.94E-03	23.65	4.53
SRXN1	sulfiredoxin 1	1.38	5.85E-02	14.25	8.19
ACADVL	acyl-CoA dehydrogenase, very long chain	1.37	2.27E-01	68.02	8.56
PSAP	prosaposin	1.37	2.61E-05	50.4	5.01
SNRPD1	small nuclear ribonucleoprotein D1 polypeptide 16kDa	1.37	5.63E-06	13.27	11.6
KRT75	keratin 75	1.36	3.20E-03	59.52	7.74
S100A6	S100 calcium binding protein A6	1.36	7.20E-06	10.17	5.48
EEF1B2	eukaryotic translation elongation factor 1 beta 2	1.35	6.96E-05	3.1	4.46
RPS19	ribosomal protein S19	1.35	7.13E-05	16.05	10.3

(*Continued*)

Table 1. (*Continued*)

HNRNPA2B1	heterogeneous nuclear ribonucleoprotein A2/B1	1.34	8.97E-05	35.98	8.65
SNRPA	small nuclear ribonucleoprotein polypeptide A	1.34	5.79E-04	31.26	9.83
AHSG	alpha-2-HS-glycoprotein	1.33	2.63E-03	39.3	5.72
HIST1H2BL	histone cluster 1, H2bl	1.33	7.96E-05	13.94	10.3
PGRMC1	progesterone receptor membrane component 1	1.33	6.83E-05	21.66	4.7
SNRPD3	small nuclear ribonucleoprotein D3 polypeptide 18kDa	1.33	1.02E-05	13.28	8.91
SRP54	signal recognition particle 54kDa	1.33	5.66E-04	48.64	9.04
VCPIP1	valosin containing protein (p97)/p47 complex interacting protein 1	1.33	3.16E-02	134.24	7.2
CLTC	clathrin, heavy chain (Hc)	1.32	3.65E-08	187.77	5.69
GOLGB1	golgin B1	1.32	1.39E-01	375.79	5
HNRNPD	heterogeneous nuclear ribonucleoprotein D (AU-rich element RNA binding protein 1, 37kDa)	1.32	2.65E-05	12.63	8.57
NES	nestin	1.32	2.46E-07	177.33	4.36
POR	P450 (cytochrome) oxidoreductase	1.32	1.28E-02	47.37	7.81
PDIA6	protein disulfide isomerase family A, member 6	1.31	1.87E-04	47.81	5.08
RPS21	ribosomal protein S21	1.31	1.07E-03	8.84	8.5
SNRPD2	small nuclear ribonucleoprotein D2 polypeptide 16.5kDa	1.31	1.55E-04	12.39	9.89
STOML2	stomatin (EPB72)-like 2	1.31	6.46E-05	33.32	8.25
GCSH	glycine cleavage system protein H (aminomethyl carrier)	1.3	1.71E-04	18.87	4.88
PRKCSH	protein kinase C substrate 80K-H	1.3	6.04E-05	59.14	4.42
RPS16	ribosomal protein S16	1.3	1.21E-03	16.44	10.2
S100P	S100 calcium binding protein P	1.3	2.54E-02	10.39	4.88
TMED2	transmembrane emp24 domain trafficking protein 2	1.3	4.88E-03	17.07	4.84
ALB	albumin	1.29	1.40E-03	51.54	6.95
ANXA11	annexin A11	1.29	2.84E-05	45.7	8.46
EIF3K	eukaryotic translation initiation factor 3, subunit K	1.29	6.97E-02	25.04	4.93
FAU	Finkel-Biskis-Reilly murine sarcoma virus (FBR-MuSV) ubiquitously expressed	1.29	1.32E-05	10.9	11.6
LETM1	leucine zipper-EF-hand containing transmembrane protein 1	1.29	7.20E-04	83.3	6.7
PDAP1	PDGFA associated protein 1	1.29	1.15E-02	4.39	10.3
PKM	pyruvate kinase, muscle	1.29	1.33E-01	58.02	7.71
PRRC1	proline-rich coiled-coil 1	1.29	5.39E-04	46.67	5.83
RAP1B	RAP1B, member of RAS oncogene family	1.29	9.51E-06	18.77	8.53
RPS10	ribosomal protein S10	1.29	1.19E-05	18.89	10.2
SERBP1	SERPINE1 mRNA binding protein 1	1.29	3.70E-04	42.4	8.44
BSG	basigin (Ok blood group)	1.28	2.34E-02	19.43	6.68
LAMTOR2	late endosomal/lysosomal adaptor, MAPK and MTOR activator 2	1.28	2.04E-03	13.5	5.4
NOLC1	nucleolar and coiled-body phosphoprotein 1	1.28	8.75E-04	73.56	9.47
PDIA3	protein disulfide isomerase family A, member 3	1.28	1.89E-06	54.07	7.21
PLCB3	phospholipase C, beta 3 (phosphatidylinositol-specific)	1.28	2.37E-06	131.12	5.88
PPIB	peptidylprolyl isomerase B (cyclophilin B)	1.28	5.59E-04	23.73	9.41
PSMB2	proteasome (prosome, macropain) subunit, beta type, 2	1.28	7.64E-04	9.55	8.78
SRSF2	serine/arginine-rich splicing factor 2	1.28	1.44E-03	23.18	11.8
CD59	CD59 molecule, complement regulatory protein	1.27	2.57E-01	11.98	5.74
ERP29	endoplasmic reticulum protein 29	1.27	1.57E-06	5.47	9.72
PDIA4	protein disulfide isomerase family A, member 4	1.27	5.23E-05	72.89	5.07
TFRC	transferrin receptor	1.27	5.69E-05	75.92	6.81
TPD52	tumor protein D52	1.27	6.66E-02	12.38	4.68
CTNNBL1	catenin, beta like 1	1.26	1.20E-01	36.08	6.7

(*Continued*)

Table 1. (*Continued*)

DBN1	drebrin 1	1.26	1.75E-03	36.45	5.14
GNG12	guanine nucleotide binding protein (G protein), gamma 12	1.26	2.68E-02	8	8.97
HRSP12	heat-responsive protein 12	1.26	3.05E-02	11.82	8.76
NPM1	nucleophosmin (nucleolar phosphoprotein B23, numatrin)	1.26	1.40E-05	29.45	4.61
OGDH	oxoglutarate (alpha-ketoglutarate) dehydrogenase (lipoamide)	1.26	3.90E-06	98.95	7.46
RPS11	ribosomal protein S11	1.26	2.43E-04	18.42	10.3
VIM	vimentin	1.26	1.15E-05	53.62	5.12
ACOT8	acyl-CoA thioesterase 8	1.25	3.28E-01	9.91	5.71
API5	apoptosis inhibitor 5	1.25	9.53E-05	48.66	5.19
EIF2A	eukaryotic translation initiation factor 2A, 65kDa	1.25	1.35E-01	35.28	8.5
HNRNPD	heterogeneous nuclear ribonucleoprotein D (AU-rich element RNA binding protein 1, 37kDa)	1.25	5.93E-03	23.06	5.11
PDIA3	protein disulfide isomerase family A, member 3	1.25	7.72E-03	13.51	7.3
PPP1R16A	protein phosphatase 1, regulatory subunit 16A	1.25	2.84E-04	57.78	6.06
ANXA5	annexin A5	1.24	4.54E-06	35.91	5.05
MRPL12	Mitochondrial Ribosomal Protein L12	1.24	3.62E-04	21.33	8.87
NAA15	N(alpha)-acetyltransferase 15, NatA auxiliary subunit	1.24	5.55E-04	86.39	6.35
PDLIM1	PDZ and LIM domain 1	1.24	1.55E-02	36.05	7.02
POFUT1	protein O-fucosyltransferase 1	1.24	1.82E-04	22.32	8.76
RAP2B	RAP2B, member of RAS oncogene family	1.24	1.31E-03	20.49	4.81
RPS28	ribosomal protein S28	1.24	7.82E-04	7.84	10.7
VPS35	vacuolar protein sorting 35 homolog (S. cerevisiae)	1.24	2.40E-01	76.16	5.43
HNRNPA1	heterogeneous nuclear ribonucleoprotein A1	1.23	1.01E-03	29.37	9.14
IDH1	isocitrate dehydrogenase 1 (NADP+), soluble	1.23	3.48E-01	46.63	7.01
MAP4	microtubule-associated protein 4	1.23	2.08E-03	120.93	5.43
RPL13	ribosomal protein L13	1.23	5.07E-04	24.25	11.7
RPS12	ribosomal protein S12	1.23	5.47E-05	14.51	7.21
RPS4X	ribosomal protein S4, X-linked	1.23	3.86E-04	29.58	10.2
EIF2S2	Eukaryotic translation initiation factor 2 subunit 2	1.22	5.59E-05	37.76	6.34
EIF5A	eukaryotic translation initiation factor 5A	1.22	6.80E-06	16.82	5.24
MYOF	myoferlin	1.22	6.17E-06	179.44	6.33
PFDN4	prefoldin subunit 4	1.22	2.21E-01	15.3	4.53
PKM	pyruvate kinase, muscle	1.22	6.68E-07	57.9	7.84
PRDX3	peroxiredoxin 3	1.22	1.59E-04	25.82	7.46
RPL27	ribosomal protein L27	1.22	7.66E-03	15.79	10.6
RPL36	ribosomal protein L36	1.22	6.74E-03	12.25	11.6
SCP2	sterol carrier protein 2	1.22	9.60E-03	13.03	5.57
SRP14	signal recognition particle 14kDa (homologous Alu RNA binding protein)	1.22	2.09E-04	14.56	10
SYNCRIP	synaptotagmin binding, cytoplasmic RNA interacting protein	1.22	1.06E-04	58.7	7.56
ALDH7A1	aldehyde dehydrogenase 7 family, member A1	1.21	6.51E-02	55.33	6.86
FH	fumarate hydratase	1.21	2.84E-05	50.18	7.4
HNRNPK	heterogeneous nuclear ribonucleoprotein K	1.21	1.03E-04	47.53	5.63
UBAP2L	ubiquitin associated protein 2-like	1.21	1.59E-01	103.11	6.87
AHNAK	AHNAK nucleoprotein	1.2	1.31E-05	628.7	6.15
ATP5G1	ATP synthase, H+ transporting, mitochondrial Fo complex, subunit C1 (subunit 9)	1.2	5.48E-01	10.19	10.4
CAB39	calcium binding protein 39	1.2	1.46E-02	39.84	6.89
DDX1	DEAD (Asp-Glu-Ala-Asp) box helicase 1	1.2	4.27E-03	69.51	7.72
NACA	nascent polypeptide-associated complex alpha subunit	1.2	2.37E-04	15.01	4.91

(*Continued*)

Table 1. (*Continued*)

Gene Symbol	Protein Name	Fold Change	P value	MW (kDa)	pI
RPS25	ribosomal protein S25	1.2	2.44E-04	13.73	10.1
S100A11	S100 calcium binding protein A11	1.2	3.27E-04	11.73	7.12
SRP9	signal recognition particle 9kDa	1.2	6.10E-04	10.11	7.97
CANX	calnexin	1.19	5.10E-05	67.53	4.6
CD55	CD55 molecule, decay accelerating factor for complement (Cromer blood group)	1.19	6.49E-04	41.2	8.03
HSPA9	heat shock 70kDa protein 9 (mortalin)	1.19	1.32E-05	72.36	5.94
MTAP	methylthioadenosine phosphorylase	1.19	2.26E-03	33.16	7.46

Downregulated Proteins

Gene Symbol	Protein Name	Fold Change	P value	MW (kDa)	pI
CDK1	cyclin-dependent kinase 1	-3.81	9.17E-05	27.49	7.06
PUF60	poly-U binding splicing factor 60KDa	-2.57	1.67E-02	26.93	8.81
NONO	non-POU domain containing, octamer-binding	-2.19	4.72E-02	23.66	9.8
HNRNPM	Heterogeneous nuclear ribonucleoprotein M	-1.95	4.40E-07	39.16	9.14
TUFM	Tu translation elongation factor, mitochondrial	-1.9	1.28E-03	49.84	7.61
ADK	adenosine kinase	-1.88	6.77E-05	38.68	6.68
ARL1	ADP-ribosylation factor-like 1	-1.86	1.92E-06	5.84	6.62
OSGEP	O-sialoglycoprotein endopeptidase	-1.84	1.60E-03	15.94	8.05
ARF1	ADP-ribosylation factor 1	-1.83	6.67E-04	20.68	6.8
HNRNPU	heterogeneous nuclear ribonucleoprotein U (scaffold attachment factor A)	-1.82	5.15E-06	83.03	8.79
PTGES3	prostaglandin E synthase 3 (cytosolic)	-1.78	1.04E-05	14.83	4.11
NSUN2	NOP2/Sun RNA methyltransferase family, member 2	-1.72	6.96E-04	59.35	6.55
LOC100508782	inositol hexakisphosphate and diphosphoinositol-pentakisphosphate kinase 1-like	-1.69	3.13E-03	91.02	7.78
TPI1	Triosephosphate isomerase	-1.68	6.05E-06	26.65	6.9
CLIC4	chloride intracellular channel 4	-1.67	8.88E-04	23.25	5.34
ENO1	enolase 1, (alpha)	-1.67	7.57E-03	36.9	6.28
WDR61	WD repeat domain 61	-1.64	2.26E-04	33.56	5.47
ARHGDIA	Rho GDP dissociation inhibitor (GDI) alpha	-1.62	2.26E-02	18.22	5.19
OTUB1	OTU domain, ubiquitin aldehyde binding 1	-1.62	1.67E-05	28.03	5.29
CMPK1	cytidine monophosphate (UMP-CMP) kinase 1, cytosolic	-1.61	1.48E-05	20.55	8.95
PRKAG1	protein kinase, AMP-activated, gamma 1 non-catalytic subunit	-1.6	1.30E-02	28.27	7.02
ARF4	ADP-ribosylation factor 4	-1.59	1.87E-05	20.5	7.14
EEF1A1	eukaryotic translation elongation factor 1 alpha 1	-1.59	4.05E-04	50.11	9.01
FDPS	farnesyl diphosphate synthase	-1.59	8.46E-05	39.63	4.98
GSTM3	glutathione S-transferase mu 3 (brain)	-1.59	5.81E-06	24.8	5.24
UBA2	ubiquitin-like modifier activating enzyme 2	-1.57	4.22E-03	60.8	5.07
SAE1	SUMO1 activating enzyme subunit 1	-1.56	5.85E-04	19.14	5.31
LRPPRC	leucine-rich pentatricopeptide repeat containing	-1.55	4.65E-05	123.2	5.54
P4HA1	prolyl 4-hydroxylase, alpha polypeptide I	-1.54	1.77E-05	58.92	6.02
LTA4H	leukotriene A4 hydrolase	-1.53	1.01E-03	57.26	6.06
COPS2	COP9 signalosome subunit 2	-1.52	1.10E-02	44.2	5.87
KIAA0196	KIAA0196	-1.52	1.95E-01	116.99	8.27
NDRG1	N-myc downstream regulated 1	-1.52	4.81E-05	38.55	6.34
APRT	adenine phosphoribosyltransferase	-1.51	6.44E-05	19.6	6.02
EIF4A3	eukaryotic translation initiation factor 4A3	-1.51	2.25E-04	46.84	6.73
NOL3	nucleolar protein 3 (apoptosis repressor with CARD domain)	-1.51	1.26E-02	24.31	11.3
PARK7	protein DJ-1	-1.51	8.34E-07	19.88	6.79
EIF6	eukaryotic translation initiation factor 6	-1.5	2.02E-03	26.58	4.68

(*Continued*)

Table 1. (*Continued*)

PCBP2	poly(rC) binding protein 2	-1.5	2.82E-05	16.99	7.69
CAMK2A	calcium/calmodulin-dependent protein kinase II alpha	-1.48	4.93E-04	2.56	9.72
PMPCA	peptidase (mitochondrial processing) alpha	-1.48	3.66E-03	28.22	6.76
PSMC6	proteasome (prosome, macropain) 26S subunit, ATPase, 6	-1.47	3.61E-04	8.7	6.11
ALDH1A3	aldehyde dehydrogenase 1 family, member A3	-1.46	1.45E-03	45.41	8.18
LGALS1	lectin, galactoside-binding, soluble, 1	-1.46	2.15E-05	14.71	5.5
TUBB	tubulin, beta class I	-1.46	8.42E-06	47.74	4.81
ALDH18A1	aldehyde dehydrogenase 18 family, member A1	-1.45	1.25E-02	87.03	7.12
KCNH3	potassium voltage-gated channel, subfamily H (eag-related), member 3	-1.45	9.78E-05	117.05	7.94
PPP2R4	protein phosphatase 2A activator, regulatory subunit 4	-1.45	1.09E-02	14.42	5.96
RAN	RAs-related Nuclear protein	-1.45	2.67E-05	24.41	7.49
RAB3IP	RAB3A interacting protein	-1.44	2.31E-04	10.27	4.68
PFN1	profilin 1	-1.43	1.09E-06	15.04	8.27
PPP1R14B	protein phosphatase 1, regulatory (inhibitor) subunit 14B	-1.43	1.02E-04	20.95	5.22
TUBB4B	tubulin, beta 4B class IVb	-1.43	3.74E-05	49.8	4.89
AP3D1	adaptor-related protein complex 3, delta 1 subunit	-1.42	1.91E-01	111.17	8.1
DDB1	damage-specific DNA binding protein 1, 127kDa	-1.42	2.08E-03	14.27	5.27
GAPDH	glyceraldehyde-3-phosphate dehydrogenase	-1.42	5.34E-06	36.03	8.46
HSP90AA1	heat shock protein 90kDa alpha (cytosolic), class A member 1	-1.42	2.19E-08	84.61	5.02
IL18	interleukin 18 (interferon-gamma-inducing factor)	-1.42	1.01E-02	22.31	4.67
MGST1	microsomal glutathione S-transferase 1	-1.42	4.37E-02	4.84	6.51
PGAM1	Phosphoglycerate Mutase 1	-1.42	3.58E-06	27.08	8.24
PGK1	phosphoglycerate kinase 1	-1.42	2.17E-05	41.4	7.33
RRM1	ribonucleotide reductase M1	-1.42	2.35E-03	86.4	6.65
SH3BGRL3	SH3 domain binding glutamic acid-rich protein like 3	-1.42	1.48E-03	9.37	9.36
SLC25A3	solute carrier family 25 (mitochondrial carrier; phosphate carrier), member 3	-1.42	1.68E-02	16.94	8.47
TALDO1	transaldolase 1	-1.42	7.90E-06	37.52	6.81
TUBA4A	tubulin, alpha 4a	-1.42	2.77E-05	48.3	5.01
DSTN	destrin (actin depolymerizing factor)	-1.41	3.16E-04	15.39	8.59
GCN1L1	GCN1 general control of amino-acid synthesis 1-like 1 (yeast)	-1.41	1.06E-03	292.57	7.47
TRIM28	tripartite motif containing 28	-1.41	3.46E-04	79.42	5.99
VAPA	VAMP (vesicle-associated membrane protein)-associated protein A, 33kDa	-1.4	3.24E-04	27.88	8.62
GSTP1	glutathione S-transferase pi 1	-1.39	1.12E-04	19.47	5.97
PRDX5	peroxiredoxin 5	-1.39	2.03E-06	17.02	7.24
PRDX6	peroxiredoxin 6	-1.39	1.85E-05	25.02	6.38
ENO1	enolase 1, (alpha)	-1.38	3.04E-07	47.14	7.39
NQO1	NAD(P)H dehydrogenase, quinone 1	-1.38	3.89E-02	22.78	8.5
PSMC1	proteasome (prosome, macropain) 26S subunit, ATPase, 1	-1.38	2.44E-04	41.14	5.01
TUBB4A	tubulin, beta 4A class IVa	-1.38	5.72E-03	49.55	4.88
UBA1	ubiquitin-like modifier activating enzyme 1	-1.38	8.03E-06	117.77	5.76
ALDH1B1	aldehyde dehydrogenase 1 family, member B1	-1.37	4.26E-05	57.17	6.8
HADHA	hydroxyacyl-CoA dehydrogenase/3-ketoacyl-CoA thiolase/enoyl-CoA hydratase (trifunctional protein), alpha subunit	-1.37	8.28E-05	82.95	9.04
SRPR	signal recognition particle receptor (docking protein)	-1.37	1.09E-02	66.52	9.04
TUBA1B	tubulin, α1b	-1.37	3.11E-05	50.12	5.06
FXR1	fragile X mental retardation, autosomal homolog 1	-1.36	2.66E-03	50.96	7.27
COTL1	coactosin-like 1 (Dictyostelium)	-1.35	3.16E-04	15.94	5.67
DDX21	DEAD (Asp-Glu-Ala-Asp) box helicase 21	-1.35	1.82E-02	79.61	9.38

(*Continued*)

Table 1. (*Continued*)

GLO1	glyoxalase I	-1.35	3.27E-03	19.03	6.05
HUWE1	HECT, UBA and WWE domain containing 1, E3 ubiquitin protein ligase	-1.35	2.91E-01	186.1	5.97
PPP1CA	protein phosphatase 1, catalytic subunit, alpha isozyme	-1.35	4.48E-06	28.88	4.87
BTF3	basic transcription factor 3	-1.34	2.36E-02	9.38	5
CALCRL	calcitonin receptor-like	-1.34	4.58E-01	54.28	6.77
CSE1L	CSE1 chromosome segregation 1-like (yeast)	-1.34	7.39E-05	107.71	5.82
FKBP1A	FK506 binding protein 1A, 12kDa	-1.34	9.10E-02	3.96	5.78
HSP90AB1	heat shock protein 90kDa alpha (cytosolic), class B member 1	-1.34	2.94E-06	83.21	5.03
PFKP	phosphofructokinase, platelet	-1.34	2.27E-03	22.66	5.2
PTMS	Parathymosin	-1.34	8.71E-03	6.25	8.12
ALDH4A1	aldehyde dehydrogenase 4 family, member A1	-1.33	7.10E-02	21.21	6.79
ALDOC	aldolase C, fructose-bisphosphate	-1.33	1.56E-04	48.38	8.07
NANS	N-acetylneuraminic acid synthase	-1.33	4.75E-03	40.28	6.74
PGM1	phosphoglucomutase 1	-1.33	2.79E-02	58.73	5.95
SFN	Stratifin	-1.33	6.47E-05	27.76	4.74
SKP1	S-phase kinase-associated protein 1	-1.33	1.80E-02	16.02	4.64
UBC	ubiquitin C	-1.33	2.23E-05	16.83	6.58
VDAC2	voltage-dependent anion channel 2	-1.33	4.75E-06	27.46	5.47
FABP5	fatty acid binding protein 5 (psoriasis-associated)	-1.32	3.47E-05	15.15	7.01
GART	Trifunctional purine biosynthetic protein adenosine-3	-1.32	8.71E-05	46	6.79
HADHB	hydroxyacyl-CoA dehydrogenase/3-ketoacyl-CoA thiolase/enoyl-CoA hydratase (trifunctional protein), beta subunit	-1.32	9.00E-04	40.39	9.79
HPRT1	hypoxanthine phosphoribosyltransferase 1	-1.32	1.60E-04	24.56	6.68
MYH9	myosin, heavy chain 9, non-muscle	-1.32	2.13E-05	226.39	5.6
PAFAH1B2	platelet-activating factor acetylhydrolase 1b, catalytic subunit 2 (30kDa)	-1.32	3.85E-03	18.35	6.27
SCCPDH	saccharopine dehydrogenase (putative)	-1.32	5.15E-01	47.12	9.14
SPAG9	sperm associated antigen 9	-1.32	1.58E-04	54.36	4.64
AK1	adenylate kinase 1	-1.31	1.24E-03	21.62	8.63
CBX1	chromobox homolog 1	-1.31	6.41E-05	19.31	5.02
EIF4A1	eukaryotic translation initiation factor 4A1	-1.31	4.59E-05	23.24	5.69
HSD17B10	hydroxysteroid (17-beta) dehydrogenase 10	-1.31	2.04E-05	26.91	7.78
PEBP1	phosphatidylethanolamine binding protein 1	-1.31	9.00E-05	21.04	7.53
ALDOA	aldolase A, fructose-bisphosphate	-1.3	3.37E-07	39.4	8.09
DDX3X	DEAD (Asp-Glu-Ala-Asp) box helicase 3, X-linked	-1.3	3.03E-05	71.31	6.62
DLAT	dihydrolipoamide S-acetyltransferase	-1.3	5.41E-04	44.57	6.2
IARS2	isoleucyl-tRNA synthetase 2, mitochondrial	-1.3	7.99E-03	113.72	7.2
COPS7B	COP9 signalosome subunit 7B	-1.29	8.77E-04	16.95	4.86
DNM1L	dynamin 1-like	-1.29	5.48E-03	64.14	7.9
EIF4A1	eukaryotic translation initiation factor 4A1	-1.29	4.34E-04	46.12	5.48
IMPDH2	IMP (inosine 5'-monophosphate) dehydrogenase 2	-1.29	3.89E-02	55.77	6.9
PSMC4	proteasome (prosome, macropain) 26S subunit, ATPase, 4	-1.29	9.56E-06	43.48	5.26
SAR1A	SAR1 homolog A (S. cerevisiae)	-1.29	5.71E-05	22.35	6.68
TLR9	toll-like receptor 9	-1.29	1.34E-04	6.27	8.5
TTLL3	tubulin tyrosine ligase-like family, member 3	-1.29	4.88E-02	49.38	8.91
UBE2M	ubiquitin-conjugating enzyme E2M	-1.29	5.04E-04	20.89	7.69
CPNE3	copine III	-1.28	4.64E-04	60.09	5.85
GTPBP3	GTP binding protein 3 (mitochondrial)	-1.28	7.61E-04	49.82	6.8
PDLIM5	PDZ and LIM domain 5	-1.28	3.05E-04	48.93	7.87

(*Continued*)

Table 1. (*Continued*)

SERPINB5	serpin peptidase inhibitor, clade B (ovalbumin), member 5	-1.28	3.26E-01	14.35	5.57
YWHAG	tyrosine 3-monooxygenase/tryptophan 5-monooxygenase activation protein, gamma polypeptide	-1.28	6.45E-04	28.28	4.89
ACOT9	acyl-CoA thioesterase 9	-1.27	3.29E-02	15.45	8.59
AKAP12	A kinase (PRKA) anchor protein 12	-1.27	1.45E-03	180.88	4.44
ATP2A2	ATPase, Ca++ transporting, cardiac muscle, slow twitch 2	-1.27	7.93E-03	109.62	5.36
CNDP2	CNDP dipeptidase 2 (metallopeptidase M20 family)	-1.27	9.58E-03	30.36	5.66
DHPS	deoxyhypusine synthase	-1.27	4.56E-03	15.08	5
EIF4H	eukaryotic translation initiation factor 4H	-1.27	3.13E-02	27.37	7.23
ERO1L	ERO1-like (S. cerevisiae)	-1.27	8.67E-04	8.82	8.69
HSDL2	hydroxysteroid dehydrogenase like 2	-1.27	6.73E-03	37.3	6.1
NASP	nuclear autoantigenic sperm protein (histone-binding)	-1.27	1.31E-02	28.18	4.23
PSMD2	proteasome (prosome, macropain) 26S subunit, non-ATPase, 2	-1.27	1.01E-03	99.25	5.16
RCN2	reticulocalbin 2, EF-hand calcium binding domain	-1.27	1.32E-01	36.85	4.4
GDI2	GDP dissociation inhibitor 2	-1.26	7.38E-05	50.63	6.47
KIF22	kinesin family member 22	-1.26	2.25E-04	66.27	8.91
PNP	purine nucleoside phosphorylase	-1.26	7.00E-04	32.53	7.21
PRKAR1A	protein kinase, cAMP-dependent, regulatory, type I, alpha	-1.26	2.72E-01	42.95	5.35
PSMC3	proteasome (prosome, macropain) 26S subunit, ATPase, 3	-1.26	7.16E-03	19.89	4.91
RNH1	ribonuclease/angiogenin inhibitor 1	-1.26	1.54E-02	20.46	4.73
UBE2L3	ubiquitin-conjugating enzyme E2L 3	-1.26	9.61E-03	14.11	8.92
KPNB1	karyopherin (importin) beta 1	-1.25	2.29E-04	97.11	4.78
MAP1S	microtubule-associated protein 1S	-1.25	3.68E-01	109.72	7.65
PPIA	peptidylprolyl isomerase A (cyclophilin A)	-1.25	3.34E-05	18	7.81
PSMD5	proteasome (prosome, macropain) 26S subunit, non-ATPase, 5	-1.25	1.49E-02	56.16	5.48
PPA1	pyrophosphatase (inorganic) 1	-1.24	7.99E-06	32.64	5.86
PYGL	phosphorylase, glycogen, liver	-1.24	3.78E-03	93.08	7.3
INF2	inverted formin, FH2 and WH2 domain containing	-1.23	8.21E-03	134.53	5.53
SSB	Sjogren syndrome antigen B (autoantigen La)	-1.23	7.67E-05	41.8	5.96
TIAM1	T-cell lymphoma invasion and metastasis 1	-1.23	1.45E-03	118.58	6.15
TRMT1	tRNA methyltransferase 1 homolog (S. cerevisiae)	-1.23	1.74E-02	69.26	7.23
XPO1	exportin 1 (CRM1 homolog, yeast)	-1.23	6.39E-06	123.31	6.06
HSPH1	heat shock 105kDa/110kDa protein 1	-1.22	5.64E-04	77.11	5.1
MIF	macrophage migration inhibitory factor (glycosylation-inhibiting factor)	-1.22	3.48E-04	12.47	7.88
PHB	Prohibitin	-1.22	3.65E-03	29.79	5.76
RPN1	ribophorin I	-1.22	1.53E-04	72.73	6.28
RPS15	ribosomal protein S15	-1.22	1.43E-03	17.03	10.4
SRM	spermidine synthase	-1.22	1.67E-03	33.8	5.49
YWHAQ	tyrosine 3-monooxygenase/tryptophan 5-monooxygenase activation protein, theta polypeptide	-1.22	2.54E-05	27.75	4.78
YWHAZ	tyrosine 3-monooxygenase/tryptophan 5-monooxygenase activation protein, zeta polypeptide	-1.22	1.33E-05	27.73	4.79
ACO2	aconitase 2, mitochondrial	-1.21	1.35E-02	54.43	7.62
ATP9A	ATPase, class II, type 9A	-1.21	1.95E-01	105.07	8.16
PPP2R1A	protein phosphatase 2, regulatory subunit A, alpha	-1.21	6.24E-06	61.48	5.12
TLN1	talin 1	-1.21	1.86E-02	257.92	6.49
CAND1	cullin-associated and neddylation-dissociated 1	-1.2	9.40E-04	136.29	5.78
ETFB	electron-transfer-flavoprotein, beta polypeptide	-1.2	1.47E-04	27.83	8.1
FKBP4	FK506 binding protein 4, 59kDa	-1.2	4.27E-03	51.77	5.43

(*Continued*)

Table 1. (*Continued*)

IQGAP1	IQ motif containing GTPase activating protein 1	-1.2	5.20E-03	189.13	6.48
MDH1	malate dehydrogenase 1, NAD (soluble)	-1.2	1.63E-02	36.4	7.36
MRPL9	mitochondrial ribosomal protein L9	-1.2	4.20E-01	17.48	10.7
MYL6	myosin, light chain 6, alkali, smooth muscle and non-muscle	-1.2	2.52E-03	11.67	4.41
NUDT21	nudix (nucleoside diphosphate linked moiety X)-type motif 21	-1.2	2.57E-01	26.21	8.82
SMS	spermine synthase	-1.2	8.92E-04	31.08	4.93

MW—Molecular Weight (kDa)

IP—Isoelectric Point

Negative numbers—downregulated; Positive numbers–upregulated

Proteins with a statistically significant fold change $\geq$ 1.2 or $\leq$ -1.2-fold were considered differentially expressed.

https://doi.org/10.1371/journal.pone.0179587.t001

confluency of the PC3 cell line was evaluated for changes in response to treatment with curcumin compared to DMSO. At 72 hrs, cells treated with 5 µg/ml of curcumin diminished their confluency when compared to DMSO (Fig 1A). To further evaluate the cytotoxicity of curcumin extract in PC3, a 7AAD assay was performed. Our results confirmed that curcumin induces approximately 40% of cell death vs 5% in DMSO (Fig 1B, p value $\leq$ 0.03). We evaluated the cell cycle effect induced by curcumin in PC3 cells, since the quantitative TMT proteomic profiling revealed differentially expressed cell cycle proteins. Cell cycle analysis revealed that curcumin treatment induced a cell cycle arrest at the G1 phase. The percentage of cells arrested in G1 was significantly higher in curcumin than DMSO (Fig 1C, p value $\leq$ 0.0020). The G0 peak was also increased under curcumin treatment and the percent of cells greater
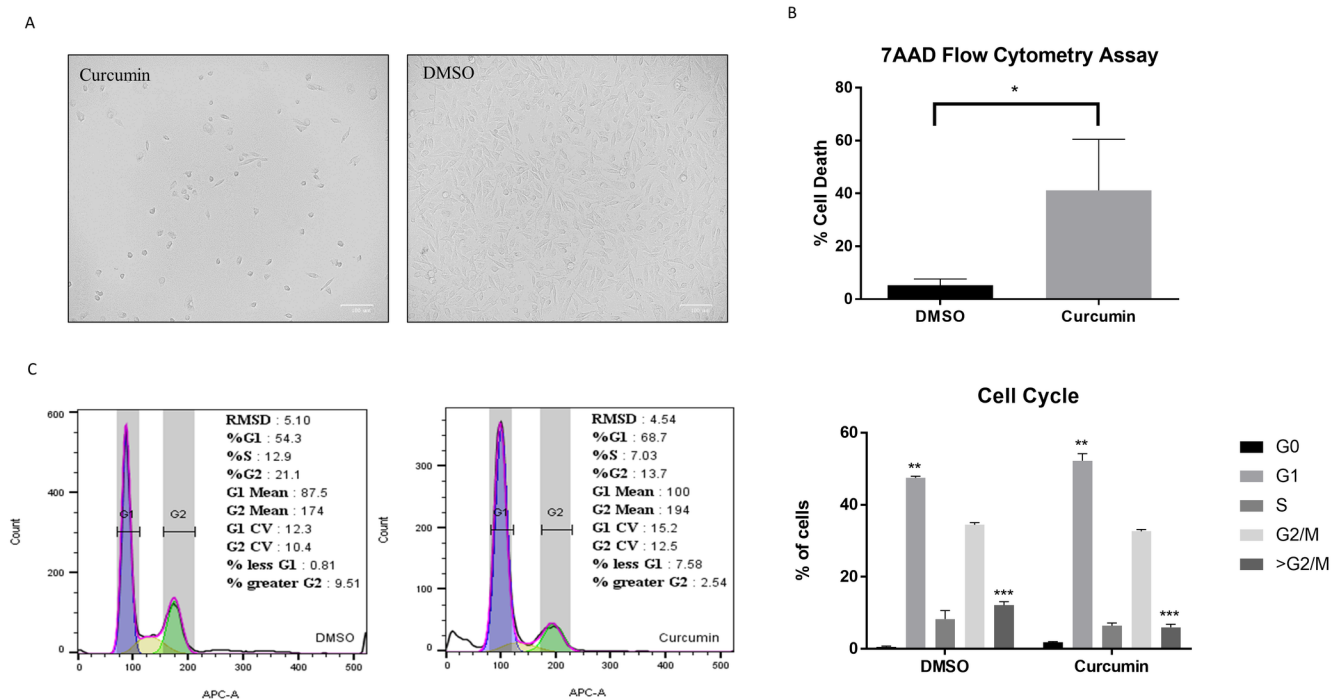
Fig 1. Curcumin inhibits cell proliferation and promotes cell death. (A) Optical micrograph of PC3 confluency after treatment with either Curcumin or DMSO. (B) Percentage of death cells stained with 7AAD, analyzed by flow cytometry and compared by unpaired t-test, p$\leq$0.05. (C) Cell cycle analysis by flow cytometry; statistical analysis was determined by Two-way ANOVA, *p$\leq$0.05, **p$\leq$0.01.

https://doi.org/10.1371/journal.pone.0179587.g001

than G2/M was significantly higher in DMSO (p value ≤ 0.0002). These results suggest that curcumin not only induces a cytotoxic effect in PC3 cells but can also deregulate the cell cycle by promoting a G0/G1 arrest.

Curcumin induces the upregulation of pro-apoptotic markers in PC3 cells

To confirm the apoptotic curcumin-induced protein alterations obtained by the quantitative proteomic results (Table 1), caspase dependent pro-apoptotic expression was evaluated to assess other cell death signaling mechanisms. Protein expression of cleaved caspase 3, an apoptotic effector protein, was evaluated using flow cytometry analysis. Approximately 17% of cells treated with curcumin exhibited cleaved caspase 3 expression when compared to 1% in DMSO (Fig 2A, p value ≤ 0.036). To validate the flow cytometry data, an ELISA assay on cells treated with curcumin or DMSO was assessed. Curcumin treated cells exhibited higher expression of cleaved caspase 3 when compared to DMSO (Fig 2B). The un-cleaved expression of caspase 3 was evaluated by qRT-PCR with a result of nearly 1.7-fold vs 1.0 in DMSO and a p-value ≤ 0.021 (Fig 2C). Caspase 9 activity was measured as a caspase initiator and upstream processor of effector caspase 3 with further apoptotic propagation. Curcumin treated cells showed an increase of 1.93-fold over DMSO (Fig 2D). Correspondingly, Poly (ADP-ribose) polymerase (PARP), a programmed cell death effector, had significantly higher expression upon curcumin treatment when compared to DMSO by means of western blot (Fig 2E, p value ≤ 0.0107). In order to further correlate the quantitative proteomic data, caspase 12 expression, a central player in ER stress induced apoptosis and cytotoxicity [21] was evaluated.
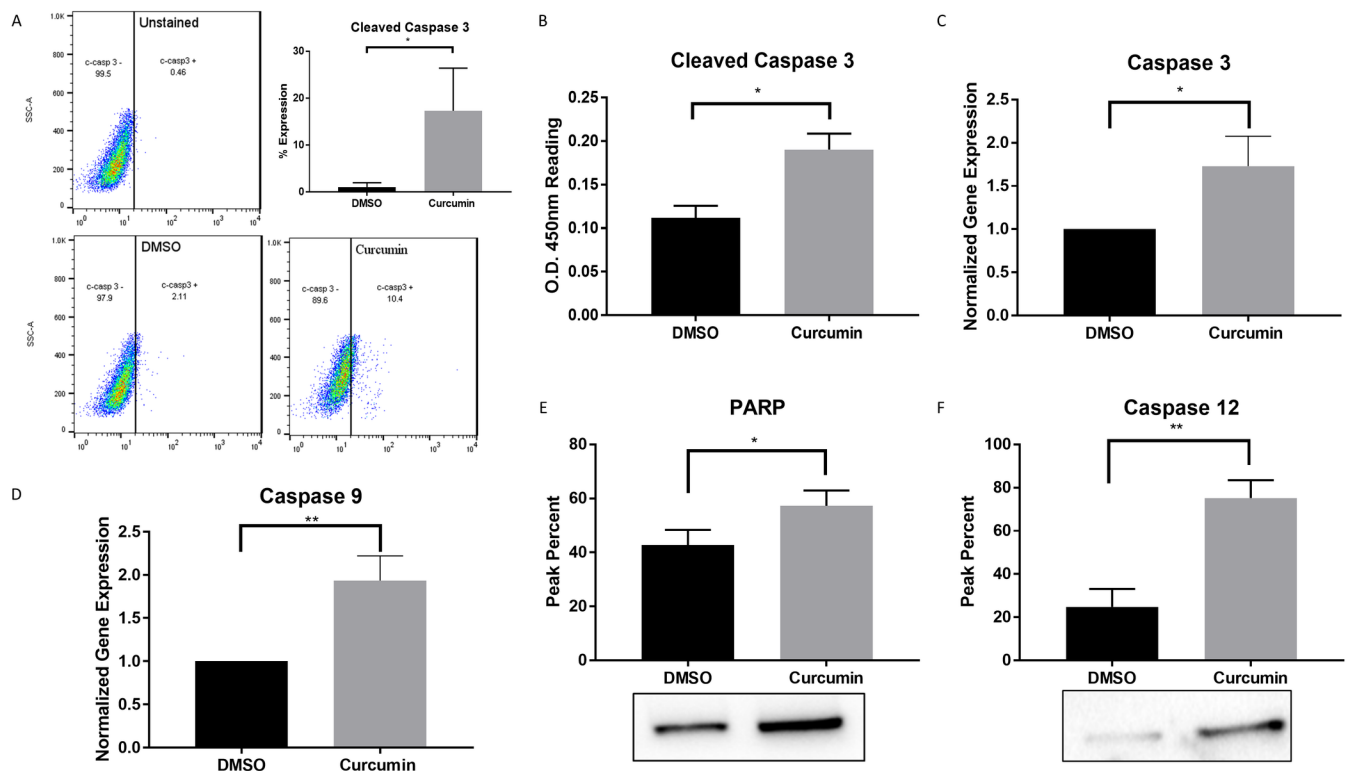
Fig 2. Curcumin induces caspase-mediated apoptosis. (A) Cleaved caspase 3 protein expression determined by flow cytometry. (B) Validation of cleaved caspase 3 protein expression by PathScan Sandwich ELISA. (C) Uncleaved caspase 3 gene expression analyzed by qRT-PCR. (D-F) Caspase 9, PARP and Caspase 12 protein expressions assessed by western blotting. Statistical significance between Curcumin and DMSO was determined by unpaired t-test, * p≤0.05, ** p≤0.01.

Curcumin PC3 treated cells induced a significantly higher expression of caspase 12 when compared to DMSO, with a peak percent in the range of 75% vs. 25% in DMSO (Fig 2F, p value ≤ 0.0017), suggesting that curcumin triggers a chronic ER stress induced cell death in prostate cancer cells.

Curcumin-induced the up regulation of ER stress markers in PC3 cells

In order to validate the ER stress curcumin-induced protein alterations obtained by the quantitative proteomics results (Table 1), cell extracts from curcumin-treated cells were analyzed by flow cytometry and western blotting. As depicted in Fig 3, curcumin treatment resulted in the upregulation of common ER stress markers GRP78, inositol-requiring enzyme 1 (Ire1α) and calreticulin (Fig 3A–3C, p value ≤ 0.0064, 0.0056 and 0.0004 respectively). Expression of p-eIF2α, a regulator in the transient translation attenuation and in the induction of apoptosis, was evaluated through flow cytometry analysis. Curcumin induced the expression of p-eIF2α by nearly 12% when compared to 6% in DMSO (Fig 3D, p value ≤ 0.0455). These results suggest that curcumin may be inducing cell death through the ER stress upstream PERK/eIF2α/ATF4 pathway in PC3 cells.

Evidences suggest that ER stress can play a key role in autophagy regulation and oxidative stress [13, 22]. To further validate the quantitative proteomics results (Table 1), curcumin's role in promoting cell death mediated chronic ER/oxidative stresses and autophagy responses were evaluated. Upon curcumin treatment, cells were exposed to 1μM of HD2CFDA for 30 minutes to determine intracellular oxidation levels. PC3 cells treated with curcumin had nearly
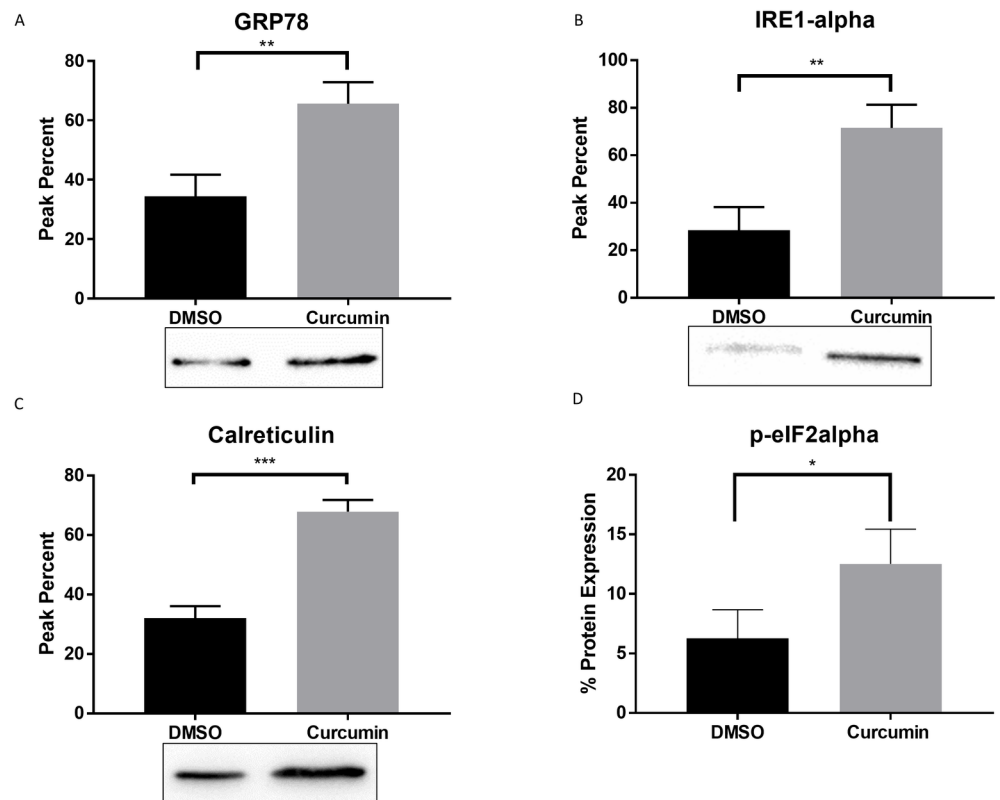
Fig 3. Curcumin triggers ER stress. (A-C) Protein expression of ER stress markers: GRP78, IRE-1α and Calreticulin analyzed by western blotting. (D) Phosphorylated expression of eIF2α protein assessed by flow cytometry. Statistical significance between Curcumin and DMSO was determined by unpaired t-test, * p≤0.05, ** p≤0.01, ***p≤0.001.

A

ROS Detection in PC3 by H₂DCFDA

B

DMSO   Curcumin

C

LC3B II

D

Total Protein
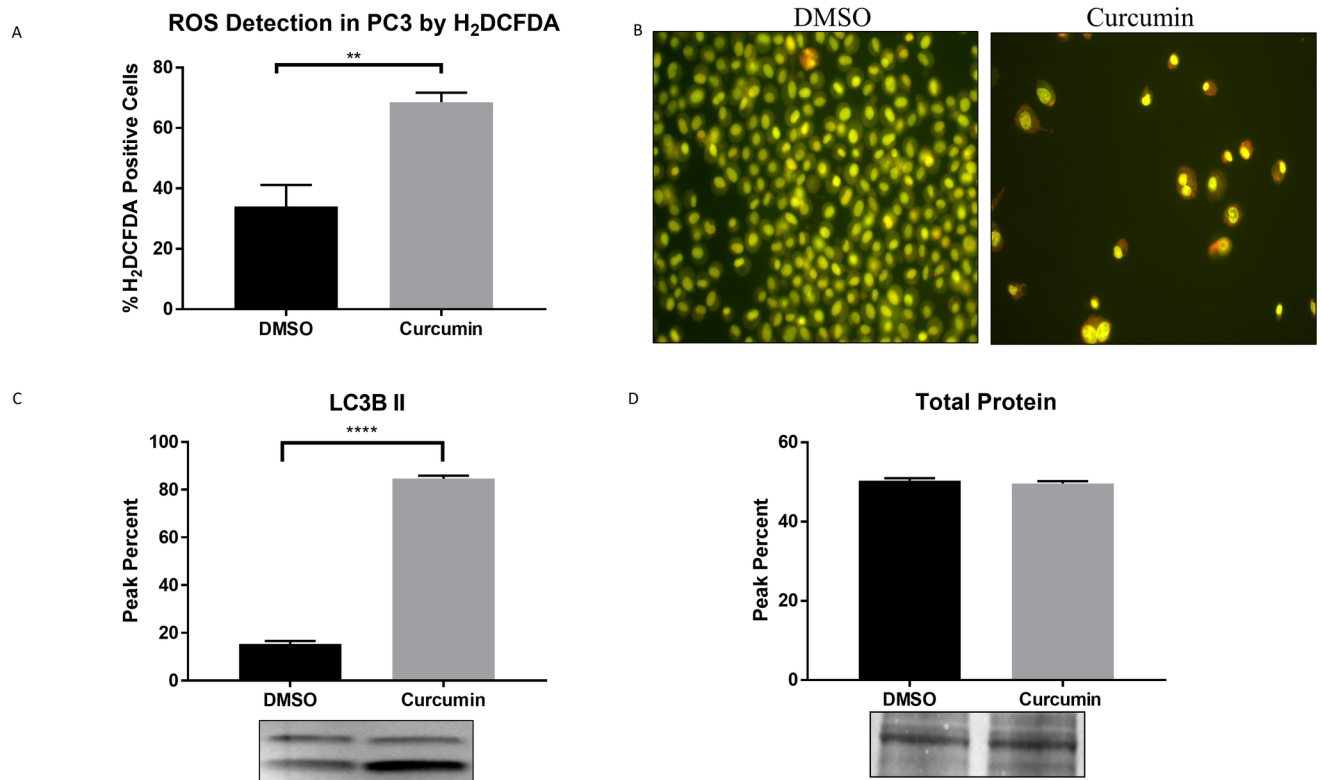
Fig 4. Curcumin promotes oxidative stress and autophagy. (A) Increased production of ROS was measured using the H₂DCFDA technique by flow cytometry. (B) Acridine orange fluorescence micrographs in curcumin and DMSO treated PC3 cells. (C) LC3B II protein expression analyzed by western blot. D. Total protein expression by india ink staining. Statistical significance between Curcumin and DMSO was determined by unpaired t-test, ** p≤0.01, **** p≤0.0001.

https://doi.org/10.1371/journal.pone.0179587.g004

70% of HD2CFDA positive cells when compared to approximately 35% cells treated with DMSO, with a p value ≤ 0.0016 (Fig 4A).

It is generally accepted that ROS induce autophagy [23], considered as a tumor suppressor mechanism by preventing ROS accumulation through elimination of damaged mitochondria. However, under prolonged or severe ER stress, apoptosis can be prompted by autophagy. To evaluate if curcumin induces autophagy, PC3 cells were treated with 5μg/mL curcumin for 72 hours and stained with acridine orange (Fig 4B). Induction of autophagy by curcumin was indicated by increased acridine orange staining due to lysosomal acidity. To confirm curcumin-induced autophagic activity, western blotting technique was used by assessing LC3B expression, a common autophagic marker. An increased level of LC3B expression with a peak percent in the range of over 80% was detected in curcumin treated PC3 cells when compared to approximately 15% in DMSO (Fig 4C, p value ≤ 0.0001).

Overall, these findings, together with the results described above, correlate with the upregulation of pro-apoptotic markers PARP and caspases 3, 9 and 12, that in turn support this study hypothesis, indicating that curcumin induces a chronic ER stress mediated cell death and activates cell cycle arrest, UPR, autophagy and oxidative stress responses.

Discussion

Anti-cancer therapies, such as chemotherapy and radiation, among others, have been shown to be aggressive approaches for treating cancer. In this study, nearly 50% of cells treated with

5 µg/ml curcumin lost viability in highly metastatic prostate cancer cells (PC3). Curcumin inhibited the growth of PC3 cells and induced a chronic ER stress and oxidative species dependent responses promoting cell death. Accumulation of misfolded proteins in the ER can disrupt ER function resulting in ER stress. The Unfolded Protein Response (UPR) functions as a cytoprotective mechanism aimed at decreasing the levels of unfolded proteins and coordinating the induction of ER chaperones with decreased protein synthesis and cell cycle growth arrest in the G1 phase. UPR activation of PERK may result in translational repression of cyclin D1, a protein required for cell cycle progression through the G1 phase, via eIF2α phosphorylation [24]. The cell cycle analysis depicted in Fig 1C revealed that curcumin caused a G0/G1 phase cell cycle arrest in PC3. Furthermore, the isobaric TMT labeling-based proteomic quantification revealed that ERp29 was overexpressed in curcumin treated cells. ERp29 is linked to PERK activation and eIF2α phosphorylation resulting in cell cycle inhibition and tumor suppression [25]. Not surprisingly, quantitative proteomic results indicate that CDK1, a key regulator of cell division, migration and inducer of mitotic cell cycle progression, was downregulated to possibly prevent cell proliferation and promote apoptosis [26, 27]. Moreover, PPP1CA, regulator of cell cycle progression and proliferation, was downregulated by -1.35-fold in curcumin treated cells [28, 29]. Thus, our results suggest that curcumin induced an UPR prompting G0/G1 cell cycle arrest.

Recent developments in the literature have demonstrated that the UPR is an important mechanism required for cancer cells to maintain malignancy. Cancer cells can adapt to ER stress and evade stress-induced apoptotic pathways by activating the UPR branches [30]. During acute ER stress, chaperone proteins are activated to correct misfolding and re-establish cellular homeostasis through the activation of the ER-associated degradation pathway. On the other hand, chronic ER stress causes UPR-mediated apoptosis. Data obtained from the quantitative proteomics TMT analysis were consistent with the cytotoxic evidence, demonstrating a strong correlation between ER stress and apoptotic markers. The proteomic data reveals that GRP78, a key ER stress marker, was upregulated in PC3 curcumin treated cells. GRP78 is a resident ER protein responsible for the regulation of the proper refolding of misfolded proteins [31]. The importance of this chaperone is directly linked to activation of the three transmembrane UPR signaling initiators: PERK, IRE1, and activating transcription factor 6. Another ER stress chaperone marker, PDI, was significantly upregulated at a fold change of 1.25 after curcumin treatment and as identified by TMT quantitative proteomics data. The PDI superfamily can act as molecular chaperones, protein-binding partners, hormone reservoirs and recently, have been implicated in the apoptotic signaling pathways [32]. Other important ER stress markers, such as calreticulin were validated through western blot analysis. This chaperone is involved in protein folding and Ca^{2+} homeostasis in the ER and can act as a proapoptotic protein under stress conditions [33]. If homeostasis cannot be reinstated by the previously mentioned pathways, the cells resort to activation of apoptosis. Another indispensable pathway involved in cellular homeostasis is the PERK–eIF2α signaling. Phosphorylated eIF2α was significantly upregulated when compared with control conditions. Upon UPR activation, eIF2α is phosphorylated by PERK to produce signaling that halts the translation of proteins in order to prevent misfolded proteins accumulation. The upregulation of eIF2α in curcumin-treated cells, suggests activation of the UPR-associated PERK pathway. Additional evidence for UPR activation is the deregulation of proteasomal proteins PMPCA, PSMB2, PSMC1 and PSMD2, demonstrating ERAD activation [34]. Under chronic ER stress settings, PERK phosphorylates eIF2α leading to the expression of transcription factor ATF4 through the PERK-eIF2α pathway. ATF4 induces the transcription of C/EBP homologous protein (CHOP, also known as GADD153) subsequently activating caspase 12 [21]. Given the important role of caspases as effector molecules in various forms of cell death including curcumin-induced apoptosis, the

ability of these anti-cancer agents to trigger caspase activation was evaluated. Caspase 12 upregulation appears to be a critical determinant of curcumin cytotoxic effect on PCa, since caspase 12 activation is an indicator of ER-stress-induced apoptosis. As extensively discussed in the literature, upon activation, caspase 12 may cleave caspase 9, which in turn activates the effector caspase 3 [35]. Caspase 3 may then cleave poly (ADP-ribose) polymerase-1 (PARP-1), involved in DNA damage and induction of programmed cell death [36]. Our results showed significantly increased expression of nearly all the proteins involved in PERK pathway such as p-eIF2α, caspase 12, 9, 3 and PARP, indicating that curcumin induced apoptosis via ER-stress. Another master regulator in cell fate determination under ER stress, IRE1, is known to initiate apoptosis via splicing of the transcription factor XBP1 and through Regulated IRE1-Dependent Decay (RIDD) activation [37]. IRE1α upregulation, supports the hypothesis that curcumin induces ER stress mediated cell death in PC3.

Likewise, the downregulation of anti-apoptotic proteins (inorganic pyrophosphatase (PPA1) and vesicle-associated membrane protein-associated protein A or VAPA) and promoting pro-apoptotic proteins, such as annexin 5 and PGRMC1 similarly lead to cell death. PPA1 enzyme has been implicated in cell survival and is essential for controlling cellular levels of inorganic pyrophosphate. Moreover, it has been proven that PPA1 silencing significantly increase cell apoptosis [38]; while, VAPA has been demonstrated to protect cells against stress-induced apoptosis. On the other hand, pro-apoptotic annexin 5, localized in the mitochondrial outer membrane, may undergo a conformational change to activate caspase 3 signaling, leading to apoptosis. Based on the quantitative proteomic data, nearly all cytoskeletal proteins (tubulin, profilin, myosin, dynamin and destrin) were downregulated in curcumin treated PC3 cells, possibly during apoptosis as demonstrated by previous evidences [39, 40]. Our findings reaffirm that the cytoskeletal reorganization plays a crucial role in cell homeostasis maintenance and execution of cell stress responses. Protein folding and chaperones ensure that only properly folded proteins exit the ER compartment. Consequently, ER calcium, alteration in the redox status or generation of ROS, and energy deprivation can affect protein folding mechanisms and ER homeostasis [41]. Both ER and oxidative stresses, through ROS generation, may prompt apoptosis under chronic stress conditions. Table 1 showed significant upregulation of oxidative stress regulators sulfiredoxin, PDZ and LIM domain protein 1, while peroxiredoxins and DJ-1 (PARK7) proteins known to lessen oxidative damage, were downregulated. Studies demonstrate that these two proteins act as protective mediators to prevent ROS-induced apoptosis[42, 43]. Imbalances between ROS and antioxidant molecules, however, result in oxidative stress. Malignant cells depend on these antioxidant mechanisms for survival as they transform, and their oncogenic activity rely on their ability to increase a cell's resistance to ROS [44]. Intracellular ROS detection by H2DCFDA showed an increased activity of oxidative species in curcumin treated cells when compared to DMSO, confirming that curcumin induced ROS and contributed to oxidative stress. Our findings establish that ROS played as an activator of cell death, since increased levels of ROS were observed while antioxidants expression was downregulated in curcumin treated cells. Subsequently, oxidant species accumulation can contribute to irreversible damage to biomolecules leading to apoptosis. These results suggest that curcumin orchestrates an apoptotic mechanism against prostate cancer cells by an ER and oxidative stress-induced apoptosis.

Autophagy, a major catabolic process which degrades and recycles proteins by engulfing autophagic substrates, can be triggered by the UPR as misfolded proteins and ROS accumulate [10]. Elevated levels of ROS activate PERK-eIF2α pathway for autophagy induction [45]. Additionally, oxidation modification results in the formation of LC3-associated autophagosomes. Curcumin induced increased expression of the LC3B autophagic marker when compared to DMSO treated cells. Moreover, Rab GDP dissociation inhibitor beta (GDI2), general regulator
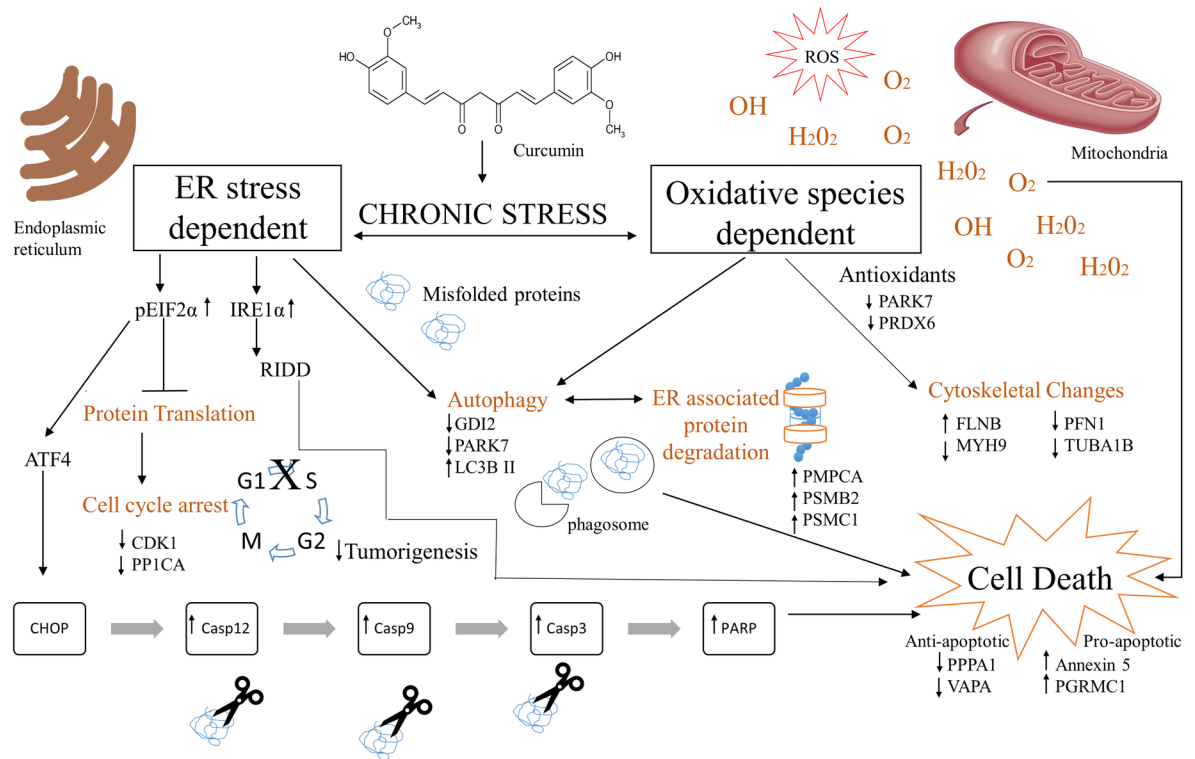
Fig 5. Proposed molecular mechanism of Curcumin's cytotoxic effects in metastatic prostate cancer cells (PC3).
Curcumin causes a chronic ER and oxidative stress inducing autophagy, cell cycle arrest, ERAD, cytoskeletal changes and caspase mediated apoptosis. Upward (↑) and downward (↓) arrows indicate upregulation or downregulation of proteins respectively.

for the membrane association of RAB proteins, was downregulated. Similar to previous observations, deregulation of GDI2 affects the activation of RAB protein, key protagonists in autophagosome formation and maturation [28, 46]. Results obtained with acridine orange staining further validate curcumin's effect on the increased autophagic activity. Cells deficient in DJ-1 (PARK7), a protein known to act in the regulation of mitochondrial function and autophagy have been shown to increase LC3 puncta and to induce higher levels of ROS [47]. Table 1 reveal that curcumin treated cells showed a DJ-1 deficiency. This could lead to multiple mitochondrial abnormalities, including decreased membrane potential, fragmented mitochondria and reduced connectivity, consequences of oxidative stress [47].

The cross-talk of ER and oxidative stress autophagic mediated apoptotic signaling observed in curcumin treated PC3 cells is shown in Fig 5. This proposed model highlights the differentially expressed proteins identified by the quantitative TMT isobaric labeling proteomic analysis and validated by qRT-PCR, western blot and flow cytometry. The upregulated proteins (upward arrows) were shown to be involved mainly in ER and oxidative stress mechanisms, autophagy, cell cycle arrest and apoptosis in curcumin treated cells. Furthermore, the results obtained suggest that ER stress proteins GRP78, PDI, calreticulin together with a set of chaperones, played a key role to activate and prompt this pro-apoptotic mechanism in PC3 cells. Moreover, curcumin induced a caspase dependent pro-apoptotic response as validated by qRT-PCR analysis. Downregulation of apoptotic proteins (downward arrows) support the anti-apoptotic/survival response obtained in DMSO treated PC3 cells. Collectively, these data provide a plausible mechanistic rationale for curcumin role in modulating major targeted cell

signaling pathways subsequently activating cell death signals inducing apoptosis in prostate cancer cells.

To our knowledge, this study is the first integrated gel-free shotgun quantitative proteomic mass spectrometry-based analysis coupled with Tandem Mass Tag isobaric labeling-based-signaling on the effect of curcumin in prostate cancer. Curcumin acted as a potent cancer growth suppressive and cytotoxic agent in PC3, via the impairment of multiple signaling mechanisms, including chronic ER stress mediated pro-apoptotic pathways. Our dataset provide insight into targets and mechanistic strategies of the anti-cancer effect of curcumin and will serve as a useful resource for future studies.

Supporting information

S1 Table. All proteins identified by TMT in curcumin and DMSO treated PC3 cells. (XLSX)

Acknowledgments

Author Contributions

Conceptualization: Nawal M. Boukli.

Data curation: Mariela Rivera, Yanilda Ramos, Jin Zou, Qiang Zhang, Guangdi Wang, Nawal M. Boukli.

Formal analysis: Mariela Rivera, Madeline Rodríguez-Valentín, Jin Zou, Nawal M. Boukli.

Funding acquisition: Jin Zou, Guangdi Wang, Nawal M. Boukli.

Investigation: Mariela Rivera, Yanilda Ramos, Madeline Rodríguez-Valentín, Sheila López-Acevedo, Jin Zou.

Methodology: Mariela Rivera, Madeline Rodríguez-Valentín, Sheila López-Acevedo, Luis A. Cubano, Jin Zou, Nawal M. Boukli.

Project administration: Nawal M. Boukli.

Resources: Luis A. Cubano, Guangdi Wang, Nawal M. Boukli.

Software: Luis A. Cubano, Guangdi Wang, Nawal M. Boukli.

Supervision: Nawal M. Boukli.

Validation: Mariela Rivera, Madeline Rodríguez-Valentín, Sheila López-Acevedo, Luis A. Cubano, Jin Zou, Nawal M. Boukli.

Visualization: Mariela Rivera, Madeline Rodríguez-Valentín, Sheila López-Acevedo, Jin Zou, Nawal M. Boukli.

Writing – original draft: Mariela Rivera, Madeline Rodríguez-Valentín, Sheila López-Acevedo, Nawal M. Boukli.

Writing – review & editing: Mariela Rivera, Nawal M. Boukli.

References

1. Siegel RL, Miller KD, Jemal A. Cancer statistics, 2016. CA: a cancer journal for clinicians. 2016; 66 (1):7–30. Epub 01/09. PMID: 26742998. https://doi.org/10.3322/caac.21332

2. Plenderleith IH. Treating the treatment: toxicity of cancer chemotherapy. Can Fam Physician. 1990; 36:1827–30. PMID: 21234006; PubMed Central PMCID: PMCPMC2280515.

3. Wu SH, Hang LW, Yang JS, Chen HY, Lin HY, Chiang JH, et al. Curcumin induces apoptosis in human non-small cell lung cancer NCI-H460 cells through ER stress and caspase cascade- and mitochondria-dependent pathways. Anticancer Res. 2010; 30(6):2125–33. PMID: 20651361.

4. Zheng R, Deng Q, Liu Y, Zhao P. Curcumin Inhibits Gastric Carcinoma Cell Growth and Induces Apoptosis by Suppressing the Wnt/beta-Catenin Signaling Pathway. Med Sci Monit. 2017; 23:163–71. PMID: 28077837. https://doi.org/10.12659/MSM.902711

5. Senft C, Polacin M, Priester M, Seifert V, Kogel D, Weissenberger J. The nontoxic natural compound Curcumin exerts anti-proliferative, anti-migratory, and anti-invasive properties against malignant gliomas. BMC Cancer. 2010; 10:491. PMID: 20840775; PubMed Central PMCID: PMCPMC2949804. https://doi.org/10.1186/1471-2407-10-491

6. Sundram V, Chauhan SC, Ebeling M, Jaggi M. Curcumin attenuates beta-catenin signaling in prostate cancer cells through activation of protein kinase D1. PLoS One. 2012; 7(4):e35368. PMID: 22523587; PubMed Central PMCID: PMCPMC3327669. https://doi.org/10.1371/journal.pone.0035368

7. Menon VP, Sudheer AR. Antioxidant and anti-inflammatory properties of curcumin. Adv Exp Med Biol. 2007; 595:105–25. PMID: 17569207. https://doi.org/10.1007/978-0-387-46401-5_3

8. Bakhshi J, Weinstein L, Poksay KS, Nishinaga B, Bredesen DE, Rao RV. Coupling endoplasmic reticulum stress to the cell death program in mouse melanoma cells: effect of curcumin. Apoptosis. 2008; 13 (7):904–14. PMID: 18493855; PubMed Central PMCID: PMCPMC2727483. https://doi.org/10.1007/s10495-008-0221-x

9. Zhao L, Ackerman SL. Endoplasmic reticulum stress in health and disease. Curr Opin Cell Biol. 2006; 18(4):444–52. PMID: 16781856. https://doi.org/10.1016/j.ceb.2006.06.005

10. Senft D, Ronai ZA. UPR, autophagy, and mitochondria crosstalk underlies the ER stress response. Trends Biochem Sci. 2015; 40(3):141–8. PMID: 25656104; PubMed Central PMCID: PMCPMC4340752. https://doi.org/10.1016/j.tibs.2015.01.002

11. Yonekawa T, Thorburn A. Autophagy and Cell Death. Essays Biochem. 2013; 55:105–17. PMID: 24070475. https://doi.org/10.1042/bse0550105

12. Cao SS, Kaufman RJ. Endoplasmic reticulum stress and oxidative stress in cell fate decision and human disease. Antioxid Redox Signal. 2014; 21(3):396–413. PMID: 24702237; PubMed Central PMCID: PMCPMC4076992. https://doi.org/10.1089/ars.2014.5851

13. Malhotra JD, Kaufman RJ. Endoplasmic reticulum stress and oxidative stress: a vicious cycle or a double-edged sword? Antioxid Redox Signal. 2007; 9(12):2277–93. PMID: 17979528. https://doi.org/10.1089/ars.2007.1782

14. Sokka AL, Putkonen N, Mudo G, Pryazhnikov E, Reijonen S, Khiroug L, et al. Endoplasmic reticulum stress inhibition protects against excitotoxic neuronal injury in the rat brain. J Neurosci. 2007; 27 (4):901–8. PMID: 17251432. https://doi.org/10.1523/JNEUROSCI.4289-06.2007

15. Eskelinen EL. The dual role of autophagy in cancer. Curr Opin Pharmacol. 2011; 11(4):294–300. PMID: 21498118. https://doi.org/10.1016/j.coph.2011.03.009

16. Kurapati KR, Samikkannu T, Kadiyala DB, Zainulabedin SM, Gandhi N, Sathaye SS, et al. Combinatorial cytotoxic effects of Curcuma longa and Zingiber officinale on the PC-3M prostate cancer cell line. J Basic Clin Physiol Pharmacol. 2012; 23(4):139–46. PMID: 23072849; PubMed Central PMCID: PMCPMC4561547. https://doi.org/10.1515/jbcpp-2012-0021

17. Rao KVK, Boukli NM, Samikkannu T, Cubano LA, Dakshayani BK, Nair M P.N. Proteomics Profiling and Cytotoxic Effect of Curcuma longa on Prostate Cancer. The Open Proteomics Journal. 2011; 4:1–11.

18. Burton LJ, Rivera M, Hawsawi O, Zou J, Hudson T, Wang G, et al. Muscadine Grape Skin Extract Induces an Unfolded Protein Response-Mediated Autophagy in Prostate Cancer Cells: A TMT-Based Quantitative Proteomic Analysis. PLoS One. 2016; 11(10):e0164115. PMID: 27755556; PubMed Central PMCID: PMCPMC5068743. https://doi.org/10.1371/journal.pone.0164115

19. Ryan D, Carberry S, Murphy AC, Lindner AU, Fay J, Hector S, et al. Calnexin, an ER-induced protein, is a prognostic marker and potential therapeutic target in colorectal cancer. J Transl Med. 2016; 14 (1):196. PMID: 27369741; PubMed Central PMCID: PMCPMC4930591. https://doi.org/10.1186/s12967-016-0948-z

20. Rhee HJ, Kim GY, Huh JW, Kim SW, Na DS. Annexin I is a stress protein induced by heat, oxidative stress and a sulfhydryl-reactive agent. Eur J Biochem. 2000; 267(11):3220–5. Epub 05/29. PMID: 10824106.

21. Nakagawa T, Zhu H, Morishima N, Li E, Xu J, Yankner BA, et al. Caspase-12 mediates endoplasmic-reticulum-specific apoptosis and cytotoxicity by amyloid-beta. Nature. 2000; 403(6765):98–103. PMID: 10638761. https://doi.org/10.1038/47513

22. Yan MM, Ni JD, Song D, Ding M, Huang J. Interplay between unfolded protein response and autophagy promotes tumor drug resistance. Oncol Lett. 2015; 10(4):1959–69. PMID: 26622781. https://doi.org/10.3892/ol.2015.3508

23. Azad MB, Chen Y, Gibson SB. Regulation of autophagy by reactive oxygen species (ROS): implications for cancer progression and treatment. Antioxid Redox Signal. 2009; 11(4):777–90. PMID: 18828708. https://doi.org/10.1089/ARS.2008.2270

24. Brewer JW, Diehl JA. PERK mediates cell-cycle exit during the mammalian unfolded protein response. Proc Natl Acad Sci U S A. 2000; 97(23):12625–30. PMID: 11035797; PubMed Central PMCID: PMCPMC18814. https://doi.org/10.1073/pnas.220247197

25. Chen S, Zhang D. Friend or foe: Endoplasmic reticulum protein 29 (ERp29) in epithelial cancer. FEBS open bio. 2015; 5:91–8. Epub 02/25. PMID: 25709888. https://doi.org/10.1016/j.fob.2015.01.004

26. Barbacid DS, Cédric B, Antonio C, Sarah H, Claudine T, Kathryn N, et al. Cdk1 is sufficient to drive the mammalian cell cycle. Nature. 2007; 448(7155):811–5. https://doi.org/10.1038/nature06046 PMID: 17700700

27. Kaldis MKD, Chandrahas Koumar R, Padmakumar VC, Tiehua D, Martin W, Vincenzo C, et al. Cyclin-dependent kinase 1 (Cdk1) is essential for cell division and suppression of DNA re-replication but not for liver regeneration. 2012. 10.1073/pnas.1115201109

28. Ao X, Zou L, Wu Y. Regulation of autophagy by the Rab GTPase network. Cell Death Differ. 2014; 21 (3):348–58. PMID: 24440914; PubMed Central PMCID: PMCPMC3921601. https://doi.org/10.1038/cdd.2013.187

29. Trinkle-Mulcahy L, Lamond AI. Mitotic phosphatases: no longer silent partners. Curr Opin Cell Biol. 2006; 18(6):623–31. PMID: 17030123. https://doi.org/10.1016/j.ceb.2006.09.001

30. Wang G, Yang ZQ, Zhang K. Endoplasmic reticulum stress response in cancer: molecular mechanism and therapeutic potential. Am J Transl Res. 2010; 2(1):65–74. PMID: 20182583; PubMed Central PMCID: PMCPMC2826823.

31. Li J, Lee AS. Stress induction of GRP78/BiP and its role in cancer. Curr Mol Med. 2006; 6(1):45–54. PMID: 16472112.

32. Grek C, Townsend DM. Protein Disulfide Isomerase Superfamily in Disease and the Regulation of Apo-ptosis. Endoplasmic Reticulum Stress Dis. 2014; 1(1):4–17. PMID: 25309899; PubMed Central PMCID: PMCPMC4192724. https://doi.org/10.2478/ersc-2013-0001

33. Lopez Sambrooks C, Carpio MA, Hallak ME. Arginylated calreticulin at plasma membrane increases susceptibility of cells to apoptosis. J Biol Chem. 2012; 287(26):22043–54. Epub 05/12. PMID: 22577148. https://doi.org/10.1074/jbc.M111.338335

34. Gomes AV. Genetics of proteasome diseases. Scientifica (Cairo). 2013; 2013:637629. PMID: 24490108; PubMed Central PMCID: PMCPMC3892944. https://doi.org/10.1155/2013/637629

35. Szegezdi E, Fitzgerald U, Samali A. Caspase-12 and ER-stress-mediated apoptosis: the story so far. Ann N Y Acad Sci. 2003; 1010:186–94. PMID: 15033718.

36. Los M, Mozoluk M, Ferrari D, Stepczynska A, Stroh C, Renz A, et al. Activation and caspase-mediated inhibition of PARP: a molecular switch between fibroblast necrosis and apoptosis in death receptor sig-naling. Mol Biol Cell. 2002; 13(3):978–88. PMID: 11907276; PubMed Central PMCID: PMCPMC99613. https://doi.org/10.1091/mbc.01-05-0272

37. Chen Y, Brandizzi F. IRE1: ER stress sensor and cell fate executor. Trends Cell Biol. 2013; 23 (11):547–55. PMID: 23880584; PubMed Central PMCID: PMCPMC3818365. https://doi.org/10.1016/j.tcb.2013.06.005

38. Lin HY, Yin Y, Zhang JX, Xuan H, Zheng Y, Zhan SS, et al. Identification of direct forkhead box O1 tar-gets involved in palmitate-induced apoptosis in clonal insulin-secreting cells using chromatin immuno-precipitation coupled to DNA selection and ligation. Diabetologia. 2012; 55(10):2703–12. PMID: 22810813. https://doi.org/10.1007/s00125-012-2643-9

39. Grzanka A, Grzanka D, Orlikowska M. Cytoskeletal reorganization during process of apoptosis induced by cytostatic drugs in K-562 and HL-60 leukemia cell lines. Biochem Pharmacol. 2003; 66(8):1611–7. PMID: 14555241.

40. Parker AL, Kavallaris M, McCarroll JA. Microtubules and Their Role in Cellular Stress in Cancer. Front Oncol. 2014; 4. PMID: 24995158. https://doi.org/10.3389/fonc.2014.00153

41. Zeeshan HM, Lee GH, Kim HR, Chae HJ. Endoplasmic Reticulum Stress and Associated ROS. Int J Mol Sci. 2016; 17(3):327. PMID: 26950115; PubMed Central PMCID: PMCPMC4813189. https://doi.org/10.3390/ijms17030327

42. Whitaker HC, Patel D, Howat WJ, Warren AY, Kay JD, Sangan T, et al. Peroxiredoxin-3 is overexpressed in prostate cancer and promotes cancer cell survival by protecting cells from oxidative stress. Br J Cancer. 2013; 109(4):983–93. PMID: 23880827; PubMed Central PMCID: PMCPMC3749568. https://doi.org/10.1038/bjc.2013.396

43. Kawate T, Iwaya K, Kikuchi R, Kaise H, Oda M, Sato E, et al. DJ-1 protein expression as a predictor of pathological complete remission after neoadjuvant chemotherapy in breast cancer patients. Breast Cancer Res Treat. 2013; 139(1):51–9. PMID: 23592371. https://doi.org/10.1007/s10549-013-2523-0

44. Kim DK, Beaven MA, Kulinski JM, Desai A, Bandara G, Bai Y, et al. Regulation of Reactive Oxygen Species and the Antioxidant Protein DJ-1 in Mastocytosis. PLoS One. 2016; 11(9):e0162831. PMID: 27611333; PubMed Central PMCID: PMCPMC5017616. https://doi.org/10.1371/journal.pone.0162831

45. Poillet-Perez L, Despouy G, Delage-Mourroux R, Boyer-Guittaut M. Interplay between ROS and autophagy in cancer cells, from tumor initiation to cancer therapy. Redox biology. 2015; 4:184–92. Epub 01/16. PMID: 25590798. https://doi.org/10.1016/j.redox.2014.12.003

46. Ullrich O, Stenmark H, Alexandrov K, Huber LA, Kaibuchi K, Sasaki T, et al. Rab GDP dissociation inhibitor as a general regulator for the membrane association of rab proteins. J Biol Chem. 1993; 268 (24):18143–50. PMID: 8349690.

47. McCoy MK, Cookson MR. DJ-1 regulation of mitochondrial function and autophagy through oxidative stress. Autophagy. 2011; 7(5):531–2. PMID: 21317550; PubMed Central PMCID: PMCPMC3127213. https://doi.org/10.4161/auto.7.5.14684